ITR…**R244** Dated 16th December 2011

Reflecting Surface of the GMRT Antennas: Design, Performance and Optimization

Govind Swarup,
National Centre for Radio Astrophysics
Tata Institute of Fundamental Research
Pune University Campus, Pune 411007.

Contents:

Reflecting Surface of the GMRT Antennas: Design, Performance and Optimization

Govind Swarup, NCRA/TIFR, Pune 411007
December 30, 2011

Summary:

The purpose of this Report is to summarize following aspects about the reflecting surface of the GMRT:

Summary in brief:

A: **Design Aspects and Performance:**

(A.1): I firstly summarize *design aspects* of the reflecting surface of the 45m diameter antennas of the Giant Metrewave Radio Telescope (GMRT) made during the late 1980s. The reflecting surface consists of stainless steel wire mesh of large spacing (low solidity; high porosity) that minimizes the wind loading on the antennas. Further, the wiremesh is supported by suitably stretched and tensioned rope trusses in order that the wiremesh forms parabolic reflecting surface of the 45m dish (SMART design: Stretched Mesh Attached to Rope Trusses) .

(A2): *Performance*: *Theodolite measurements* of the rms errors of the reflecting surface of the GMRT 45m dishes made during 1993-95 have shown that there are much larger deviations of the reflecting surface than were specified to the Contractors in 1989. In this Report I discuss practicality of correcting these deviations that would result in significant increase of the effective collecting area of the dishes by > 20% at the L band (in addition to improvements as discussed in Section B).

(A3): The GMRT maintenance engineers are planning to *replace the rusted galvanized turnbuckle that are* connected to the tensioned rope trusses, supporting the wiremesh, by stainless steel units developed by them. Also, certain other urgent repairs need to be carried out to the tubular members of the parabolic frames of 4 or more antennas

B: **Proposed Improvements**

(B1): I examine in this Report a *proposal for replacing the existing wiremesh* of 10mm x 10mm mesh in the central 1/3rd area, 15mm x 15 mm in the middle 1/3rd area and 20mm x 20mm in the outer 1/3rd area with a *wiremesh of smaller spacing* of 6mm x 6mm mesh in the central 1/3rd area, 10mm x 10 mm in the middle 1/3rd area and 15mm x 15mm for the outer 1/3rd area. Recent measurements of the drag factors, C_d and consequent wind loading are discussed in this Report in detail, suggesting that the proposed replacement would not lead to undue increase of stresses in the structural members, but this aspect would need to be examined in more detail by a structural engineer using a computer aided analysis.

(B2) I also suggest that *a new L band feed may be planned* that would result in appreciable increase in the sensitivity of the 45m dishes. A better L band feed, installing wiremesh of smaller spacing and ensuring lower RMS errors would result in increase of the sensitivity of the GMRT by a factor of ~1.8 at L band (say 800 MHz to 1430 MHz), and operation even up to 1700 MHz or more.

C: Next Plan

(C): It would be highly desirable to make the above changes in the next few years in a systematic way. This will continue to make the GMRT highly competitive internationally (including the major changes that are already being carried out concerning the Electronics and Correlator system). These changes on the reflector surface of the 45m antennas are major jobs and would need a suitable contractor. One may initially plan replacement of the wiremesh for one or two sectors out of the 16 sectors of one of the 45m dishes by the GMRT maintenance group, supplemented by a gang of contract workers. If the above proposals summarized in the above paragraphs A and B are considered important, I suggest a budget of at least ~ Rs 6 or 7 crores in the 12th plan for improving the reflecting surface of the GMRT antennas, as well ***to increase reliability of the structural and mechanical parts of the dishes for a life of more than 30 years from now.*** No doubt the engineering groups of the GMRT are doing excellent work for the maintenance of the 30 antennas of 45m diameter; it is not easy and they need all the support. Nevertheless, a well documented maintenance schedule with periodic monitoring and a monthly documented summary of changes made and planned should be submitted to the Chief Scientist, Dean and the Centre Director. A formal monthly and yearly summary is highly desirable in my view. Tata Consulting Engineers (TCE) was asked to do periodic monitoring and write a periodic report but I am told that it has not been satisfactory. ***(I must add that I retired from the GMRT/NCRA long ago, and this note has been written only as an academic exercise. I hope that it would be taken in that spirit only).***

May I also point here that the projected annual maintenance of the new ASKAP in Australia consisting of about 36 parabolic dishes of 12m diameter is projected as Aus $ 12.2 million x Rs. 53.8 = Rs. 650 crores! **ASKAP has Al sheet reflectors and a wide field of view using a Phased array operating in the frequency range of 700 MHz to 1.8 GHz, with a target to extend it up to 2.5 GHz. But the GMRT would have a much larger collecting area in the L band after its upgrading at a relatively modest cost, apart from its wide frequency coverage at metre and dcm wavelengths.**

Detailed Summary

I give below a longer summary of the proposals listed in paragraphs (A) to (C) in the above brief summary. Further details are given in the main text of this Report. I may note that I plan to write another report regarding the *pointing errors* of the GMRT antennas, considering the design of various sub-systems, performance and possible improvements.

A: Design aspects and performance:

The reflecting surface of the 45m diameter dishes of the GMRT consists of stainless steel wire mesh of 10mm x 10mm size for the inner one third area of the dishes, 15mm x 15mm for the middle one third area and 20mm x 20mm x 0.55mm for the outer one third area. The mesh is made of stainless (s.s.) wires of 0.55 mm diameter. The mesh is supported by a system of rope trusses of 4mm diameter that are connected and stretched under tension between adjacent 16 parabolic frames of the 45m dishes (Fig. 1). The reflecting surface is not a perfect parabolic surface and consists of ~900 plain panels with relatively small rms errors with respect to the required parabolic surface. This design called SMART (Stretched Mesh Attached to Rope Trusses) was selected by us in order to minimize wind loading, yet achieving good reflectance to the incoming radio waves from celestial radio sources at metre and decimeter wavelengths.

It may be noted that wind loads are the key and major factors in the cost of a parabolic dish. The SMART design suggested by me in May 1986 resulted in considerable economy and allowed construction of 30 nos. of 45m parabolic dish at affordable cost (the total cost of the GMRT project during 1988 to 1996, including antennas, electronics, optical fibre network, civil works and salaries was only Rs 45 crores, equal to only US$ 16 million, at the exchange rate prevalent during the period! I may add that it was not easy to get funds from the Government due to the great financial constraints occurring in India during 1980s and early 90s, prior to the economical liberation in 1992. Therefore, we had to optimize the design and cost of the structural parts, mechanical drive system and electronics of the 45m dishes. If the GMRT project is built today, my estimate is that it would cost at least Rs 200 crores! It would be prudent to invest modest funds of, say, only Rs 6 or 7 crores or somewhat more for improving the surface accuracy and taking steps to ensure the safety and reliability of the structural and mechanical parts of the GMRT for a further period of 30 years or more. It may be noted that the Jodrell Bank radio telescope of 76m diameter is more than 62 years old and has been upgraded several times; Parkes Radio Telescope of 65m diameter has celebrated its 50th year on October 31st 2011 and 530m X 30m Ooty Radio Telescope is over 41 years old and still going strong! Major efforts for a major upgrade of the electronics system of the GMRT are already in progress by the GMRT scientists and engineers. (It may not be out of place to note here that, in contrast, the cost of the proposed National Solar Telescope of 2 m diameter to be imported by IIA is likely to be more than Rs. 300 crores).

During construction of the 45m dishes, surface deviations of +/- 8mm for the 10mm x 10mm mesh, +/- 12mm for the 15mm x 15mm mesh and +/- 15mm for the 20mm x 20mm mesh were specified, including the design and likely fabrication errors based on our experience on a prototype 45m dish constructed at the RAC, Ooty. After the 30 nos. of 45m antennas were constructed at the GMRT sites, surface deviations were measured for ~ 6000 points of each of the 30 antennas using a theodolite during 1993-94. **Large errors were noted in most antennas**, exceeding the above specifications. These errors have resulted in lower efficiencies for most of the antennas, some even by a factor of 1.5, with an average efficiency of ~ 80% at the wavelength of 21cm. Calculations of the L band efficiencies for 21 no. of 45m dishes made by G. Sankar of the GMRT group are summarized by me in this Report for 21 antennas. It should be noted, however, that the surface deviations do not decrease the efficiencies significantly at the lower frequencies, as their adverse effect is inversely proportional to the square of the wavelength.

Recently, the engineering maintenance group of the GMRT has found that the turnbuckles used for stretching the 4mm diameter rope trusses supporting the wire mesh have got rusted in almost all antennas. In some cases the ropes have been detached from the parabolic frames and had to be re-attached. It has been proposed by the GMRT mechanical engineering group to replace all the ~1200 turnbuckles of each of the 30 nos. of the 45m antennas by stainless steel units. Surface errors would need to be corrected at the same time. It has already been done for 2 out of the 16 sectors of one of the 45m antenna. Replacing turnbuckles is a major job indeed, requiring a well defined written procedure ensuring design stress in the rope trusses and measuring coordinates of the nodes at the PRFs and two points on the rope trusses using a theodolite. I may point that practicality of carrying out corrections of the GMRT surface has been ably demonstrated by the GMRT maintenance group, by adopting an ingenious method in which a net was stretched just below the adjacent parabolic frames of one of the 16 sectors of the 45m dish. This enabled carrying out the above job at heights of ~ 25m to 35m conveniently and safely. Also, I understand that holes have been noted in the tubes of the parabolic frames of 4 antennas, which have been covered by a sleeve. *All the above jobs and any other mechanical job etc. could be carried out at the same time by a major contractor.*

B: Proposed Improvements

I also describe in this Report a proposal for replacing the existing wire meshes by changing the entire surface by 6mm x 6mm for the inner one third areas of the dishes, 10mm x 10mm for the middle one third areas and 15mm x 15mm for the outer one third areas. It will result in higher reflectivity of the wiremesh and also lower contribution by the ground radiation (lower value of receiver noise), resulting in an increase in the efficiencies of the GMRT antennas at a wavelength of 21 cm by about 20%. Further, correcting the rms errors of the present reflecting surface would also increase the efficiency by more than 20%. The above replacement would also allow operation of the GMRT antennas up to 1.7 GHz or even up to higher frequencies. In order to evaluate the proposed replacement of the wire mesh,, I discuss in detail recent data about the wind drag factors, C_d , of the wire-mesh that show appreciably lower values than those used in the original design by the TCE. As discussed in some detail in this Report, recent measurements of C_d show that the proposed replacement of the existing wire mesh by a wire mesh of smaller spacing will not result in a significant increase in the wind loads and resulting stresses in the structural members, but it would need a detailed computer based examination by a structural engineer. Also, if wire meshes are replaced, it should be possible to design smaller turnbuckles at a much lower cost.

I conclude by suggesting that all the above jobs can be carried out within two months for each 45m antenna by a team of about 30 to 35 workers, by their working at the same time on 4 out of 16 sectors every two weeks (with 6 or 7 workers per sector and some additional workers and supervisors, etc.). By releasing two antennas for retrofitting at a time, the entire job can be done for 30 antennas in 30 months by a suitable contractor, maximum 3 years including down time during monsoon. The job does not require great competence but requires appropriate organizational skill and commitment of a Contractor. It seems important to me to seek adequate funds in the 12th plan for the above job that will make the GMRT internationally competitive for decades to come, in addition to upgrades being done regarding the electronic systems. No doubt, the GMRT is one of the nation's jewels in the field of basic sciences. A major upgrade has been

done for many of the radio telescopes in the world every 20 years or so, not only for the electronic system, but also regarding the structural and mechanical aspects.

Three of the thirty GMRT antennas have close spacing of about 90m. These spacing do not provide significant information for mapping celestial radio sources of less than about 10 arc minutes, as visibilities are suitably weighted during making radio maps for such sources. For such projects, two of the 3 antennas could be used independently for pulsar observations, etc. Hence, more expensive cooled receivers could be installed in 2 or all these 3 antennas. Can we make at least one of these three 45m antennas of much better quality, including installing a phased array on one of the three over the next few years?

1 Introduction

In ***Section 2*** are discussed basic design aspects of the GMRT antennas, particularly the innovative design of the reflecting surface. In ***Section 3***, are presented details of the rms deviation of the reflecting surface of the GMRT 45m dishes, based on theodolite measurements made on ~ 6000 points of each of the 45m dishes during 1993-95. As described therein, rms deviations of the wire-mesh are unfortunately quite large for many of the antennas. As discussed in ***Section 4***, these errors have resulted in poor 'RMS efficiency' of the 30 antennas of the GMRT, with average efficiency of ~ 80% at 1420 MHz.

In ***Section 5***, I firstly summarize factors that contribute to the wind loads on the wire mesh of the reflecting surface. In particular I describe the wind drag factors, C_d , that were used by the Tata Consulting Engineers (TCE) for the design of the 45 m dishes during 1988-1991, based on data available in the literature at that time. I then describe recently available information that shows much lower drag factors by the wind velocity on the wire mesh. Therefore, as discussed in **Section 6,** it seems possible to change the existing wire meshes of sizes 10mmx10mm x 0.55mm, 15mmx15mmx 0.55mm and 20x20mmx 0.55mm for the inner 1/3rd area, middle 1/3rd and outer 1/3rd areas respectively by 6mmx6mmx0.55mm, 10mmx10mmx0.55mm and 15mmx15mmx0.55mm for the inner, middle and outer 1/3rd areas respectively. An improved computer analysis, including possibly a Computer fluid Dynamic (CFD) software to evaluate shielding of various structural members may be done to examine the possibility of using a finer wiremesh as suggested in Section 6. The above improvements will allow operation of the GMRT up to 1.7 GHz or even higher. In ***Section 7*** are summarized various factors such as taper efficiency, illumination efficiency, polarization loss, Body of Revolution (BOR) loss, return loss and RMS errors that contribute to Efficiency of a parabolidal antenna. I also compare various feed alternatives for the L band of the GMRT. Conclusions are given in ***Section 8.***

2 Basic Design Aspects of the 45m Dishes and of the Reflecting Surface

It became possible to construct the 45 m diameter antenna of the GMRT highly economically (within the available budget) by deciding to use firstly (a) wire mesh of low solidity (high porosity) that minimizes wind loads and yet provides good performance at metre and decimeter

wavelengths and (b) by an innovation to connect the wire mesh to stretched rope trusses as described below. The reflecting surface of the 45m diameter parabolic dish antennas of the GMRT consists of stainless steel wire mesh of size 10mm x 10mm for the inner one third areas of the dishes, 15mm x 15mm for the middle one third areas and 20mm x 20mm for the outer one third areas. The mesh is made of stainless (ss) wires of 0.55 mm diameter. The mesh is supported by a system of rope trusses of 4mm diameter connected under tension to the circular tubes of 16 parabolic frames of the GMRT 45m dishes. The 4 mm rope trusses are stretched between adjacent parabolic frames every 1.2 m apart and then pulled back by two ropes connected to the bottom of the parabolic frames, so that 2 nodes on the parabolic frames and two intermediate nodes at the top rope trusses lie on the surface of the 45m parabolic dish (Fig. 1).

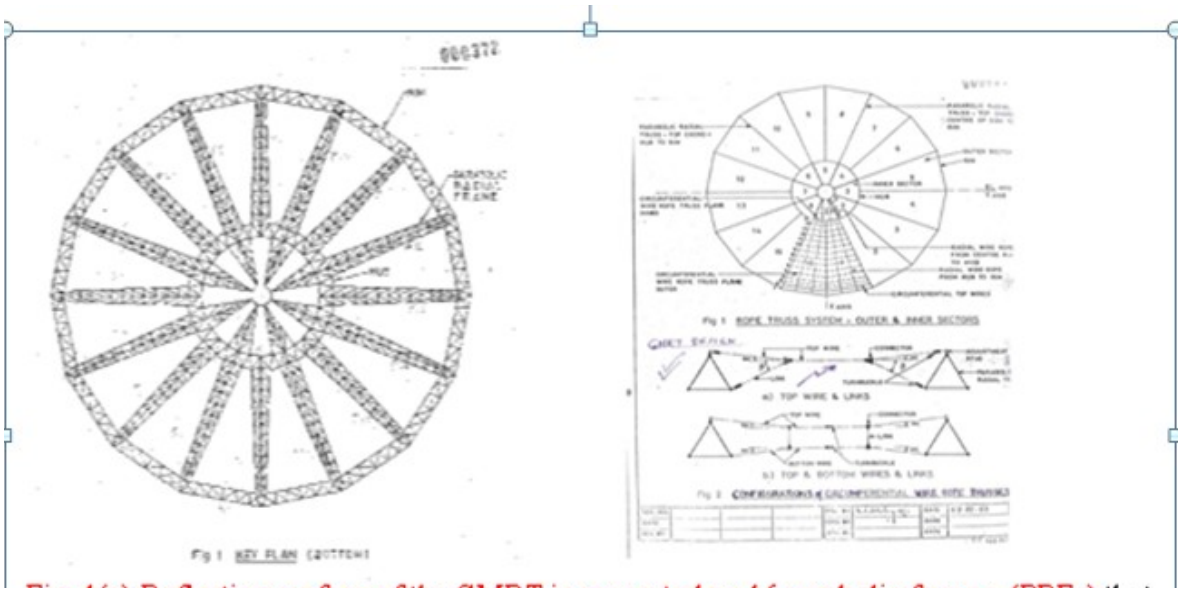

Fig.1(a): On left is shown a Plan showing 16 parabolic frames, (PRFs) of the 45 m dish, that are connected at the outer end to 16 RIMs, and on inner side to a central HUB. The HUB is connected to to a cradle (not shown here) that is palced on two elevation bearings palced on a Yoke.

Fig. 1(b): On the right is shown connestion of the reflecting surface. The outer part of each PRF from the Hub to the Rim consists of 16 sections. At each of the 16 sections, stretched ropes are connected between adjacent PRFs, as shown in the middle part of the Fig 1(b) marked by a double tick, and finally the wire meshes are stretched and connected to the rope trusses. The configuration shown in the bottom of Fig. 1(b) (on right side) was not adopted because of the possibility of oscillations of the stretched rope trusses..

Thus, the reflecting surface is not a perfect parabolic surface but consists of ~900 plane panels with acceptable rms error of the surface. This design, called SMART (Stretched Mesh Attached to Rope Trusses), was selected by us in order to minimize the wind loading, yet achieving good reflectance of the incoming radio waves from celestial radio sources at metre and decimeter wavelengths. It may be noted that wind loads are the main factor in the cost of a parabolic dish. This unique design suggested by me in May 1986 resulted in considerable economy and allowed construction of 30 nos. of 45m parabolic dish at affordable cost (even then, it was not easy to get funds from the Government due to considerable financial constraints during late 1980s and early 90s).

3 Measurements of the RMS Errors of the Reflecting Surface of the 45m Dishes constructed during 1990-1996.

3.1 *Contract specifications regarding surface accuracy:* The 30 nos. of 45m dishes were constructed during 1990- 1996. Fifteen antennas were constructed by M/s V.M. Jog Engineering Ltd. (VMJ) of Pune and another fifteen by M/s Southern Structural Ltd. (SSL) of Madras. As per the Contract, VMJ and SSL were asked to use an appropriate method using a theodolite for ensuring that the nodes at the top of the parabolic frames and two intermediate support points of each of the stretched rope truss (see Section 2, Fig. 1) lie at specified coordinates on a paraboloid of f/d = 185240/45000 = 0.412. Calculated values for these nodes by TCE were given to the Contactors as per the tender drawings and specifications. The wire meshes to be attached to the stretched rope trusses by appropriate pulling and tying with a thin wire were specified to be wrinkle free. Thus, the wire meshes for each resulting panel were expected to be close to the surface of the 45m diameter paraboloid, within the specified acceptable errors. The Contract provided that any departures from the required paraboloid of the 45m dishes should be within *+/- 8mm for the inner 1/3rd area* that has 10mmx10mm mesh, *+/- 12mm for the middle 1/3rd area* with the15mmx15mm mesh and *+/- 20mm for the outer 1/ 3rd area* with the 20mmx20mm mesh. Thus, the estimated rms errors were expected as ~ 4.7mm, 7.9mm and 12.0 mm for each of the 16 sectors of the 45m dish (including the relatively smaller values due to the departure of the wiremesh panels between each node from a true paraboloidal surface).

3.2 *Construction steps for the 45m dishes*: The erection process was briefly as follows: (1) firstly, the Concrete towers forming pedestal of the 45m dish was constructed, (2) next the Yoke made of steel plates was fabricated and erected on the ~ 4m diameter Azimuth Bearing that was bolted to the top of the Concrete tower, (3) next a Cradle made of structurally welded tubes, including the elevation gear sector, was connected to the Yoke by placing it on two Plummer blocks containing spherical bearings attached to the cradle; (2) simultaneously the outer structural part of each of the 45m dish, including the Hub, was assembled on the ground by welding individual tubular members; (it may be noted that the outer part of the dish was assembled surrounding the central concrete tower, for the sake of economy because building the dish elsewhere and lifting it using cranes would have been costly); rope trusses were then connected to the parabolic frames of the outer part of the dish, tensioned and adjusted suitably using a theodolite so that their nodes lie on a parabolic surface; soon after the wire meshes forming the reflecting surface were attached to the rope trusses; (3) finally, the outer portion of the 45m dish was lifted using winches, with ropes connected to 4 corners of the Hub; the outer part of the dish was then bolted to the Cradle; the wiremesh surface was then built inside the 12m diameter of the Hub, thus completing the 45 m dish. Finally the mechanical, electrical, electronic and servo systems were installed.

During construction of the antennas during the period 1991-1996, nodes at the parabolic frames consisting of adjustable blocks and also the two intermediate support points of each of rope trusses were required to be adjusted by the two Contactors to be within few mm of the required coordinates using a theodolite. Small beads were attached every few meters apart on the wiremesh to be able to measure the surface errors subsequently after erection of the dish.

3.3 *Survey:* After all the dishes were erected, 6000 points were surveyed in 1994 on each dish using a theodolite placed at the apex of the dish, and readings recorded digitally on a laptop. The data for 21 dishes was later analyzed by G. Sankar of the GMRT group who calculated deviations from best fit paraboloid for each antenna. After the last 9 antennas were measured, the laptop fell to the ground. Sankar may be able to retrieve data for the other 9 dishes that were surveyed again later.

4 Relative Efficiency of the GMRT Antennas at 1420 due to RMS errors

4.1 *Average Loss due to rms errors*: In this section are presented results of the rms deviation of the reflecting surface of the GMRT 45m dishes, based on measurements made during 1993-95. *As described in Section 4(c), rms deviations of the wire-mesh are unfortunately are quite large for many of the antennas, resulting in their lower efficiency, varying from about 97% to 36% with average loss of 20% at 1420 MHz.*

4.2 *Loss of sensitivity due to the surface errors:* Efficiency factor, η due to the rms errors, ρ, may be defined as the ratio of the achieved Directivity, $D = 4\pi A_{eff} / \lambda^2$ of the antenna compared to the theoretical value D_0, whence $\eta = D/D_0 = (1/(1+ \text{variance } \rho)) \approx (1- \rho)^2$ for $\rho << 1$, where $\rho = 2\cos\theta \times 2\pi\delta/\lambda$, with δ being mean rms surface error (a factor $2\cos\theta$, before 2π arises as the reflected ray at angle θ with respect to the normal suffers twice the path of the surface error) and λ is wavelength (Bracewell, 1961; Ruze, 1955). For larger errors, one should use the exponential factor given by Ruze. One should also weight the rms errors over the parabolic dish by the radiation pattern of the primary feed.

4.3 *Efficiency factor η at 1420 MHz*: In Table I(a) are presented calculated values of the ratio of the efficiency factor η at 1420 MHz, due to the measured surface errors for 14 out of the 15 antennas, constructed by VMJ, relative to the efficiency factor η for the case if rms errors were within the specifications as per the contract. This table is based on the calculations made by G. Sankar. He estimated the overall efficiency as 48.1%, considering the radiation pattern of the L band feed developed by RRI and *the specified RMS errors of the reflecting surface as per the Contract. Table I(b) gives the same for 7 out of 15 antennas built by M/s Southern Structural Limited (SSL).*

Col. 1 of Table I(a), gives antenna number. Col. 2 gives measured rms errors for 14 antennas of the GMRT constructed by VMJ. The rms errors have been calculated based on measurements made on 6000 points. In the **first row** of the Col. 2 of Table I (a) are given estimated rms errors if peak to peak deviations were the same as specified in the Contract. In Row 1, G. Sankar has given overall efficiency as 0.481 for the specified rms errors, including consideration of spillover and taper efficiencies. Colums 3, 4 and 5 give relative efficiencies. Col. 3 gives estimated overall efficiency based on measured rms errors, spillover and taper efficiencies. In Col. 4, Sankar estimates the efficiency factor due to the rms errors as 0.889 at 21cm wavelength, corresponding to the weighted rms error, δ = 6mm (Section 4.2). Column 5 gives relative efficiency due to the rms errors with respect to the contract value. [I assume that Sankar had calculated effective area of the antennas at L band as 0.541 [= (0.481/0.889)] x true area of a 45m dish (= $\pi.45^2/4$ = 1590m^2) = 0.541 x 1590m^2 = 860 m^2, considering spillover and taper also. However, I may note

that A Raghunathan who designed the L band feed had concluded in his thesis, based on his measurements of the feed that the overall efficiency of the GMRT antennas, as only 0.33 rather than 0.481 assumed by Sankar (see Section 7)].

4.4 *RMS efficiencies:* To summarize, the above paragraph, the last column of Table I (a) gives relative RMS efficiencies at 1420 MHz for 14 out of the 15 antennas constructed by M/s V. M. J. Engineering Ltd., based on measured deviations over ~ 6000 points from a true paraboloid using a theodolite. An efficiency of 100% is assumed if the RMS errors were within those specified in the Contract (this Table is tabulated by G. Swarup from that made by G. Sankar of the GMRT group).

It is seen that the antennas C3, C4, C9, W5, E4 and E6 have much lower efficiency, varying from ~ 55% to 84%. The overall relative efficiency is ~ 80%, implying the average value of the effecting collecting area, A_{eff} , of these 14 antennas as 0.481 X 0.8 x π $45^2/4$ = 611m^2. However, if we consider the value of the efficiency given by Raghunathan as 0.33 (see Section 7), the average value of the collecting area at L band = 419 m^2. As discussed in Sections 7 and 8, it should be possible to improve the overall efficiency of the GMRT at L band by a factor of 1.8 or even 2. I suggest measurement of the effective area, A_{eff} of the dishes by pointing to the Moon at L band. The Moon has a diameter of ~ 31 arc minute but the 45m dishes has beam of only ~ 21 arc minute. Since the brightness temperature of the Moon is known to be ~ 230K, this method should give accurate value of A_{eff} , rather than depending on Noise temperature calibration that does not include antenna losses etc. Even at 610 MHz, observation towards the Moon would improve present estimates of efficiencies of 45m dishes.

Table I (a) gives relative RMS efficiencies at 1420 MHz of 14 out of 15 antennas constructed by M/s V. M. J. Engineering Ltd., based on measured deviations over ~ 6000 points from a true paraboloid using a theodolite. Col. 1 gives antenna no., Col. 2 measured RMS errors, Col. 3 overall efficiency η, Col. 4 relative efficiency with respect to the ideal case as per contract specifications, Col. 5 percentage efficiency.

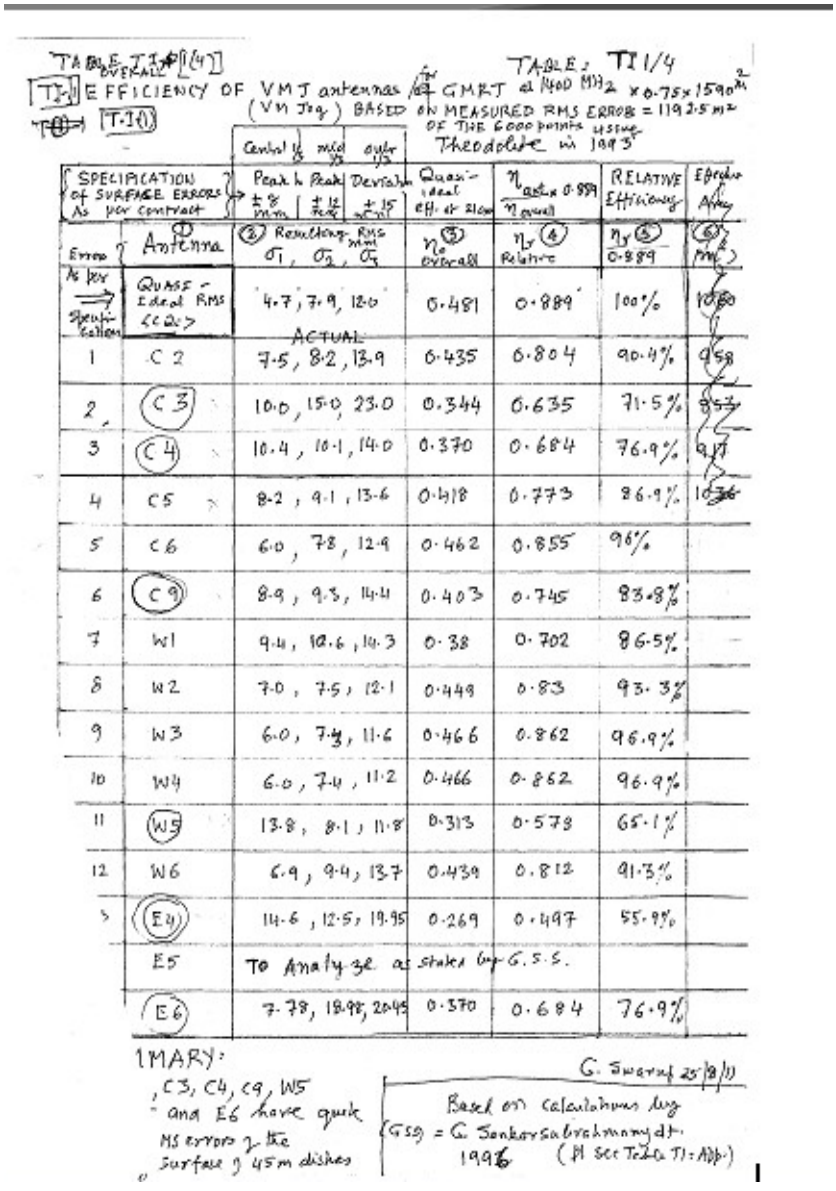

TABLE I (a) [4]

EFFICIENCY OF VMJ antennas (VM Jrg) @ GMRT at 1400 MHz $\times 0.75 \times 1590\ m^2$ BASED ON MEASURED RMS ERROR = 1192.5 m^2 OF THE 6000 points using Theodolite in 1995

SPECIFICATION of SURFACE ERRORS As per contract		Central 1/3 Peak to Peak ± 8 mm	mid 1/3 Peak to Peak ± 12 mm	outer 1/3 Deviation ± 15 mm	Quasi-ideal eff. or 21cm	$\eta_{ant} \times 0.989$ / $\eta_{overall}$	RELATIVE Efficiency	Effective Area
Error As per Specification	Antenna	(2) Resulting RMS mm $\sigma_1, \sigma_2, \sigma_3$	η_o overall (3)	η_r (4) Relative	η_r (5) 0.989	(6) %		
	QUASE - Ideal RMS <c2>	4.7, 7.9, 12.0	0.481	0.889	100%	1080		
		ACTUAL						
1	C 2	7.5, 8.2, 13.9	0.435	0.804	90.4%	958		
2	C 3	10.0, 15.0, 23.0	0.344	0.635	71.5%	857		
3	C 4	10.4, 10.1, 14.0	0.370	0.684	76.9%	917		
4	C 5	8.2, 9.1, 13.6	0.418	0.773	86.9%	1036		
5	C 6	6.0, 7.8, 12.9	0.462	0.855	96%			
6	C 9	8.9, 9.3, 14.4	0.403	0.745	83.8%			
7	W 1	9.4, 10.6, 14.3	0.38	0.702	86.5%			
8	W 2	7.0, 7.5, 12.1	0.449	0.83	93.3%			
9	W 3	6.0, 7.3, 11.6	0.466	0.862	96.9%			
10	W 4	6.0, 7.4, 11.2	0.466	0.862	96.9%			
11	W 5	13.8, 8.1, 11.8	0.313	0.578	65.1%			
12	W 6	6.9, 9.4, 13.7	0.439	0.812	91.3%			
13	E 4	14.6, 12.5, 19.95	0.269	0.497	55.9%			
	E 5	To Analyse as stated by G.S.S.						
	E 6	7.78, 18.98, 20.45	0.370	0.684	76.9%			

SUMMARY:
, C3, C4, C9, W5
" and E6 have quite
MS errors & the
surface of 45m dishes

G. Swarup 25/8/11

Based on calculations by
(GSS) & G. Sankarasubramanyam dt.
1998 (Pl see Tech Rep T1: Appx.)

We illustrate in the following Table T1b, the basis for the data in Table Ia) which is based on the reflecting surface deviations from a true paraboloid for one of the 16 sectors of the C9 antenna, as measured by a theodolite survey and tabulated by G. Sankar. It is seen that deviations are much larger than the peak to peak deviations specified in the Contract.

Table I(b): gives as a typical example of the surface deviations from a true paraboloid of 27 points across the adjacent parabolic frames of the Sector 1-2 of the C9 antenna that was constructed by VMJ. Measurements were done by a surveyor of NCRA, using a theodolite and reduced by G. Sankar. Sector 1-2 is one of the 16 sectors of the full 45m dish. Points marked as R1-1 and R9-3 refer to values measured on and near the adjustable blocks of the parabolic frames. R4-1 and R7-1 give deviations at the anchor points of the rope trusses (see Fig. 1). On the right side are given specified values as per the contract. It is seen that many values marked by shadowing are much larger than the values as per contract specifications resulting in reduced efficiency of the 45m dish.

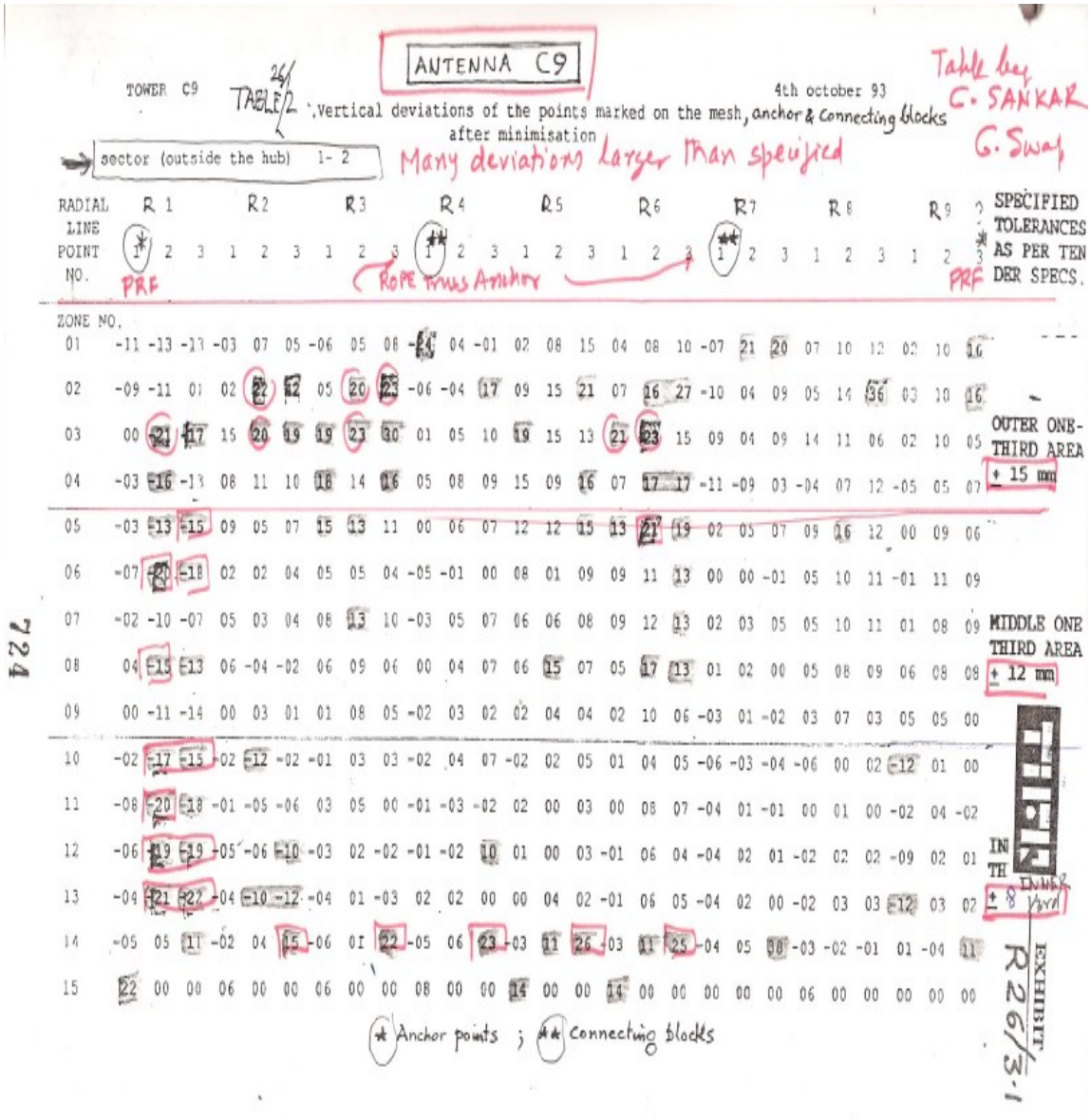
ANTENNA C9

TOWER C9 TABLE/2 4th october 93

Vertical deviations of the points marked on the mesh, anchor & Connecting blocks after minimisation

Table by C. SANKAR G. Swamy

sector (outside the hub) 1- 2

Many deviations larger than specified

RADIAL LINE POINT NO.	R1 1	R1 2	R1 3	R2 1	R2 2	R2 3	R3 1	R3 2	R3 3	R4 1	R4 2	R4 3	R5 1	R5 2	R5 3	R6 1	R6 2	R6 3	R7 1	R7 2	R7 3	R8 1	R8 2	R8 3	R9 1	R9 2	R9 3	SPECIFIED TOLERANCES AS PER TENDER SPECS.
ZONE NO.																												
01	-11	-13	-13	-03	07	05	-06	05	08	-14	04	-01	02	08	15	04	08	10	-07	21	20	07	10	12	02	10	16	
02	-09	-11	01	02	22	12	05	20	23	-06	-04	17	09	15	21	07	16	27	-10	04	09	05	14	36	03	10	16	
03	00	21	17	15	20	19	19	23	30	01	05	10	19	15	13	21	23	15	09	04	09	14	11	06	02	10	05	OUTER ONE-THIRD AREA
04	-03	-16	-13	08	11	10	18	14	16	05	08	09	15	09	16	07	17	17	-11	-09	03	-04	07	12	-05	05	07	± 15 mm
05	-03	-13	-15	09	05	07	15	13	11	00	06	07	12	12	15	13	21	19	02	05	07	09	16	12	00	09	06	
06	-07	-20	-18	02	02	04	05	05	04	-05	-01	00	08	01	09	09	11	13	00	00	-01	05	10	11	-01	11	09	
07	-02	-10	-07	05	03	04	08	13	10	-03	05	07	06	06	08	09	12	13	02	03	05	05	10	11	01	08	09	MIDDLE ONE THIRD AREA
08	04	-15	-13	06	-04	-02	06	09	06	00	04	07	06	15	07	05	17	13	01	02	00	05	08	09	06	08	08	± 12 mm
09	00	-11	-14	00	03	01	01	08	05	-02	03	02	02	04	04	02	10	06	-03	01	-02	03	07	03	05	05	00	
10	-02	-17	-15	-02	-12	-02	-01	03	03	-02	04	07	-02	02	05	01	04	05	-06	-03	-04	-06	00	02	-12	01	00	
11	-08	-20	-18	-01	-05	-06	03	05	00	-01	-03	-02	02	00	03	00	08	07	-04	01	-01	00	01	00	-02	04	-02	
12	-06	-19	-19	-05	-06	-10	-03	02	-02	-01	-02	10	01	00	03	-01	06	04	-04	02	01	-02	02	02	-09	02	01	IN TH
13	-04	-21	-22	-04	-10	-12	-04	01	-03	02	02	00	00	04	02	-01	06	05	-04	02	00	-02	03	03	-12	03	02	± 8 mm
14	-05	05	11	-02	04	15	-06	01	22	-05	06	23	-03	11	26	03	11	25	-04	05	30	-03	-02	-01	01	-04	11	
15	22	00	00	06	00	00	06	00	00	08	00	00	14	00	00	14	00	00	00	00	00	06	00	00	00	00	00	

(*) Anchor points ; (**) Connecting blocks

724

EXHIBIT R 26/3-1

Table I(c): RMS Efficiencies of 7 out of 15 antennas constructed by M/s Structural Steel Ltd., Madras (now Chennai).

Note on SSL antennas' Efficiency

G. Sankar 27th DEC. 1996

The computed efficiency (@ 1400 MHz) for the SSL antennas - viz. C1, C8, C8, E3, C10, C13 & C14 (seven) are furnished in the table. The rms values of inner, middle & outer 1/3rd area sections are also provided.

Efficiency computation takes into account the surface errors, mesh-leakage, blockage & scattering losses of feed-turret and quadripod legs. The values are compared with a quasi-ideal antenna having surface rms's of 4.7, 7.9 & 12.0 (or having deviations of ±8, ±12 & ±15 mm) and the relative efficiency is also given (i.e. 100% for Quasi-ideal case ...)

Antenna	Sigma's of inner, middle & outer segments	Efficiency $\eta_{overall}$ (@1400 MHz)	Relative to* Quasi-ideal (%)
C1	8.4, 8.9, 12.6	0.417	86.7%
C8	6.9, 9.2, 13.4	0.441	91.7%
C8	7.9, 8.3, 13.2	0.428	89.0%
E3	9.9, 10.4, 14.1	0.379	78.8%
C10	13.3, 14.7, 16.5	0.283	58.9%
C13	18.9, 15.6, 17.0	0.175	36.4%
C14	10.4, 10.8, 14.3	0.366	76.1%

* Quasi-ideal antenna's efficiency @ 1400 MHz = 0.481

In Fig. 2(a) and Fig. 2(b) are presented histograms of relative efficiency of 14 VMJ and 7 SSL antennas respectively

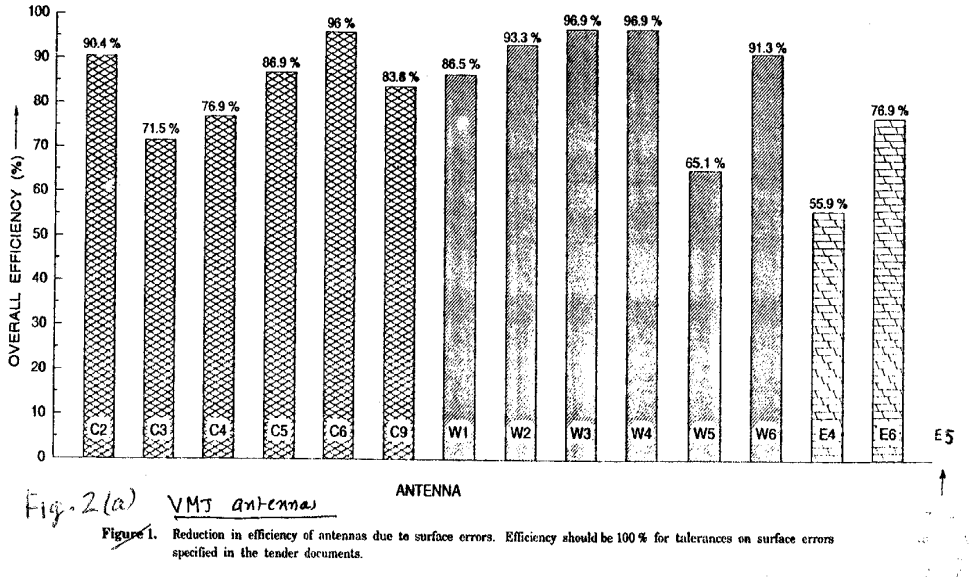

Fig. 2(a) Relative Efficiency at 1420 MHz of 14 out of 15 antennas constructed by VMJ; it may be seen that the antennas C3, C4, W5 and E4 have relative efficiency < 80% due to large RMS errors of the surface (see Table 1(a).

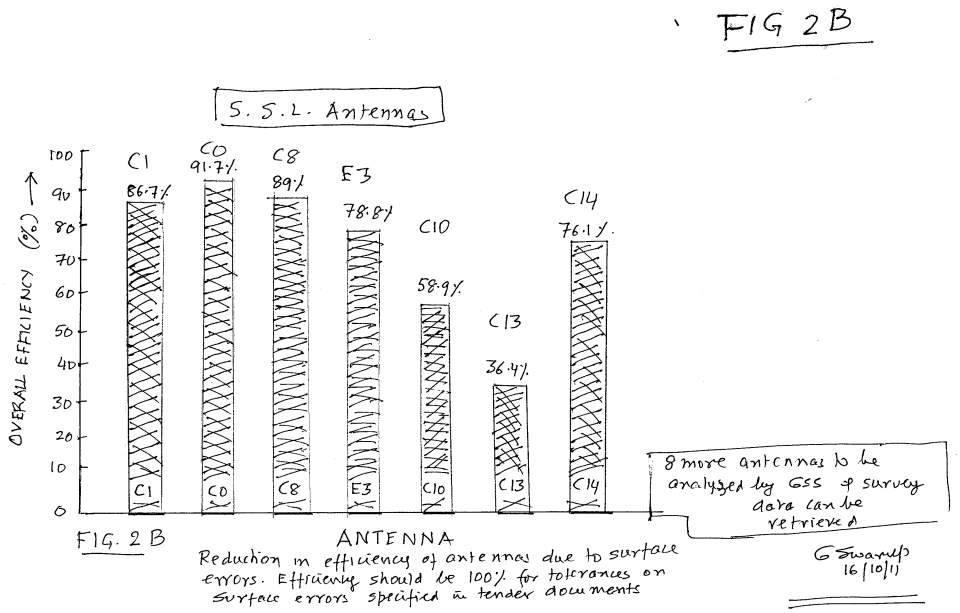

Fig. 2(b) Relative Efficiency at 1420 MHz of 7 out of 15 antennas constructed by SSL; it may be seen that the antennas E3, C10 and C13 have relative efficiency < 80% due to large RMS errors of the surface, with C13 being only ~36%! (see Table 1(b)).

4.5 ***Summary of Relative efficiencies:*** **The relative efficiencies of the 14 VMJ antennas vary from 96% to 56% (Table Ia and Fig. 2a), and for the 7 SSL antennas from 92% to 36% (Table Ib and Fig. 2b). The overall relative efficiency is ~ 80%, implying that the average value of the effective collecting area, A_{eff} ,of these 21 antennas is only 0.481 X 0.8 x π $45^2/4 = 611 m^2$. However, if we consider the value of the efficiency given by Raghunathaan as 0.33 (see text), the average value of the collecting area at L band = 419 m^2. It will be interesting to compare these values with respect to the effective areas, A_{eff}, or Gain, $G_1 = (A_{eff} /2k)$,or $G_2 = 4\pi (A_{eff} /\lambda^2)$ that has been measured by astronomers for the GMRT antennas at or near 1420 MHz (see Section 4.4).**

5 Wind Loads on the Reflecting Surface of the 45m Dishes.

5.1 *Wind Loads*: It is known that wind loads are the major contributor to the cost of a parabolic dish by a large factor (except at mm wavelengths whence surface errors and gravitational deviation of the dish due to its rotation also play a major factor in the design of a parabolic dish antenna). Hence, in order to be able to construct the 45 m dishes for operation at dcm and meter wavelengths within available funds, it was decided to use sparse wiremesh with low solidity for the reflecting surface of the 45m dishes. As stated earlier, the reflecting surface of the GMRT antennas consists of stainless steel wiremesh of size 10mm x 10mm for the inner one third areas of the dishes, 15mm x 15mm for the middle one third areas and 20mm x 20mm for the outer one third areas. The mesh was made of stainless (s.s.) wires of 0.55 mm diameter that are spot welded to make the square wiremesh. The mesh was manufactured specially for the GMRT project by M/s Evergreen Ltd., Bombay.

Wind force, F = W(v) , on a paraboloidal antenna in the direction of the wind is given by (Cohen and Vellozzi, 1964; ESDU 1984; Janardan et al. 1990):

$$F = W(v) = \tfrac{1}{2} \rho v^2 A C_d , \qquad \text{(Eq. 1)}$$

where ρ is mean air density (kg/m^3), v (m/s) is wind velocity, A (m^2) is area of the dish ($\pi d^2/4$) and C_d is a drag factor in the wind direction. The factor $\tfrac{1}{2} \rho v^2$ is the wind pressure. At sea level, ρ = 1.23 kg/ m^3. At the height of 600m of the location of the GMRT, a value of ρ = 1.106 was assumed by TCE (Janardhan et al. 1990); v is maximum wind velocity expected during the assumed life time of the antenna, called the survival wind velocity. A period of 50 year was considered as the expected life of the GMRT antennas, for which the survival wind velocity was assumed as 133kmph = 37m/s, based on maximum velocities observed at Pune during 1948 to 1990 (Kapahi and Swarup 1986). However, for the Pune region, Indian Standard Institutions (IS875) has recommended a value of 39m/s (implying 11% additional stresses). At the Pune Airport, even somewhat higher values have been reported. I have discussed these aspects in detail in the Internal Technical Report ITR 236 in the NCRA library Swarup2007). In that report, I have also summarized maximum stresses on some of the structural members of the GMRT, as calculated by TCE for the design value of wind velocity = 37m/s.

As stressed in ITR236, it is EXTREMELY important that the GMRT antennas are stowlocked when the 3 second wind velocity exceeds 50 km/s (preferably 1 minute average 45km/s), particularly during the thunderstorm period of 15th March to 15th June and the

month of September each year. (I plan to write another ITR summarizing the wind data at Pune over the last 60 years.)

5.2 Wind Load on wire mesh surfaces

Wind load, W(v), on the wire mesh of solidity S is given by

$$W(v) = A.S.\ C_d .1/2\ \rho(v)^2 , \qquad \text{Eq.(2)}$$

where ρ is the air density, v is the air velocity in m/s, A is the total surface area of the mesh, C_d is the wind drag factor being a function of the solidity of the mesh, S is its solidity, $S=[1-(w-d)^2/w^2]$; w is the width of each face of the square mesh and d is diameter of the wire; the value of ρ was taken as ~1.106 kg/m^2 by TCE for the GMRT site having 600m height above the sea level (Janardan et al. 1990).

C_d is also dependant on the Reynolds number, Re. For d ~ 0.5 to 1 mm, the values of Re range from about 1000 to ~15000 for wind velocity of about 10 m/s to ~50 m/s. However, C_d does not vary appreciably with Re values in that range (see Richards and Robinson 1999 and other data in the literature).

5.3 Drag factors of the wire meshes used for the GMRT:

In 1987, measurements were made at the National Aeronautical Laboratory (NAL) at Bangalore for various sizes of wire mesh that were planned for the GMRT. However, TCE decided to use only the upper bound of published values that were available in 1988, although these values were for the wire meshes *of appreciably higher solidity* than those used for the GMRT (Consulting engineers naturally insist to use only available national codes or published values). Curve no. 5 in Fig. 3 of the present Report shows the C_d values used by TCE as a function of the incidence angle of the wind. The curves A, B and C show the measurements made by Jayaraman (1987) based on wind tunnel measurements made at the National Aeronautical laboratory (NAL), Bangalore and those A*, B* and C* by Sivaramakrishnan et al. (1988) of NAL. Wind tunnel measurements on a 6mm x 6mm x 0.55mm wiremesh made by Lakshman et al. (2008) on a request by NCRA are also shown as Curve D in Fig. 3. They used a large modern wind tunnel facility at the Structural Engineering Research Centre of CSIR (SERC) at Chennai.

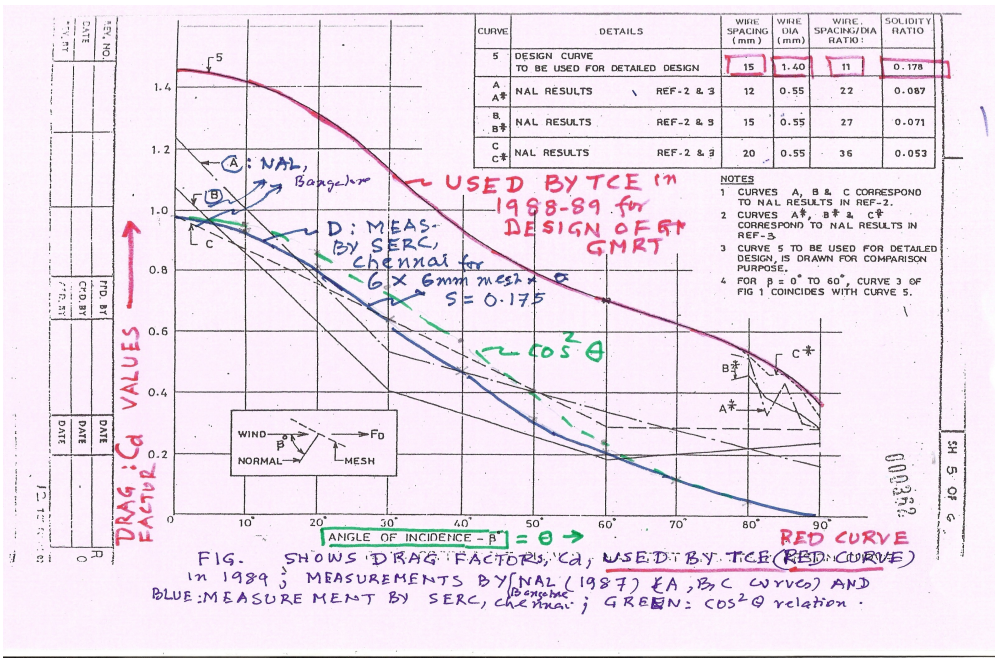

Fig.3: Curve marked as 5 (red) shows variation of the Wind drag factor, C_d with angle of incidence of the wind as adopted by TCE for **all the three wiremesh of the GMRT**, with value at normal incidence to the mesh as $C_d \sim 1.45$. Curves, A, B and C (black) show wind tunnel measurements made at NAL, Bangalore in 1987. Curve D (blue) shows wind tunnel measurements made at SERC, Chennai, on a wiremesh of size 6mm x 6mm x 0.55mm, showing that the value of $C_d = 1.0$ at normal incidence, and $\text{Cos}^2\,\theta$ variation (green): (see Fig. 4).

Fig. 4 shows the derived curves by SERC of the drag factor C_d, lift coefficient C_l and resultant C_r.

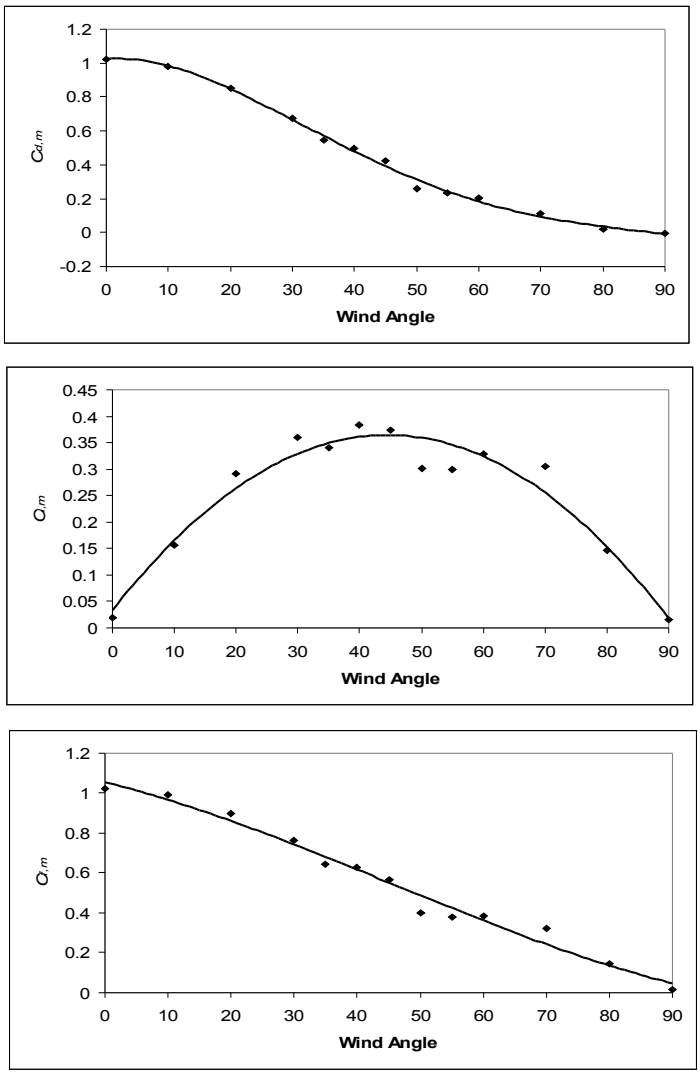

Fig. 4: Measurement of the drag factor, C_d, lift factor C_l and resultant C_f by Lakshmanan et al. (2008) of SERC, Chennai.

5.4 *Comparison of measured values of C_d with values derived by an equation by Richard and Robinson:* In 2007, I did a literature survey and found a paper by Richard and Robinson (RR 1999) from New Zealand, who had compiled published data and some of their measurements for wire mesh panels of different solidity, S. They noted (Fig. 5a), that the variation of C_d with angle of incidence, θ, show values in between Cos θ and Cos^2 θ variation, compared to Cos θ variation as per measurements by SERC (see top part of Fig. 4).

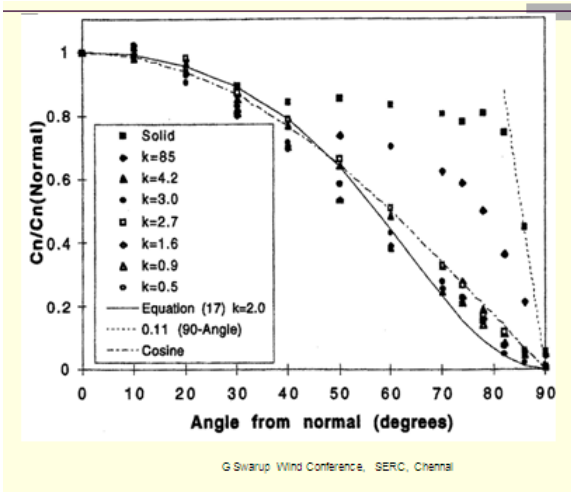

Fig. 5(a): plotted by Richard and Robinson (1999) shows that C_d has a dependence between Cos θ and Cos^2 θ.

Richard and Robinson (RR 1999) plotted all available data in the literature and found that the loss coefficient k of the wind velocity for round wire meshes (= C_d.S of this report) has a non-linear relation with k decreasing rapidly for wire meshes of higher porosity (i.e. lower solidity) as shown in Fig. 5(b). As can be derived by comparing relations in the present report with those in their paper, solidity, $S = [1-(w-d)^2/w^2] = (1-\beta)$, where β is the porosity.

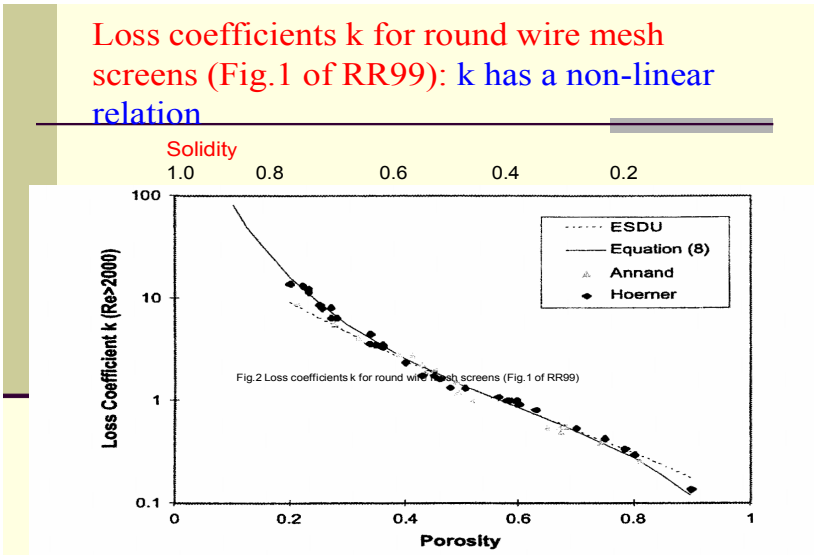

Fig. 5(b). Loss coefficients k for round wire mesh screen (Fig. 1 of RR99).

RR 99 derived an equation fitting all the published data for wire mesh panels of different porosity as given in Fig. 5(c).

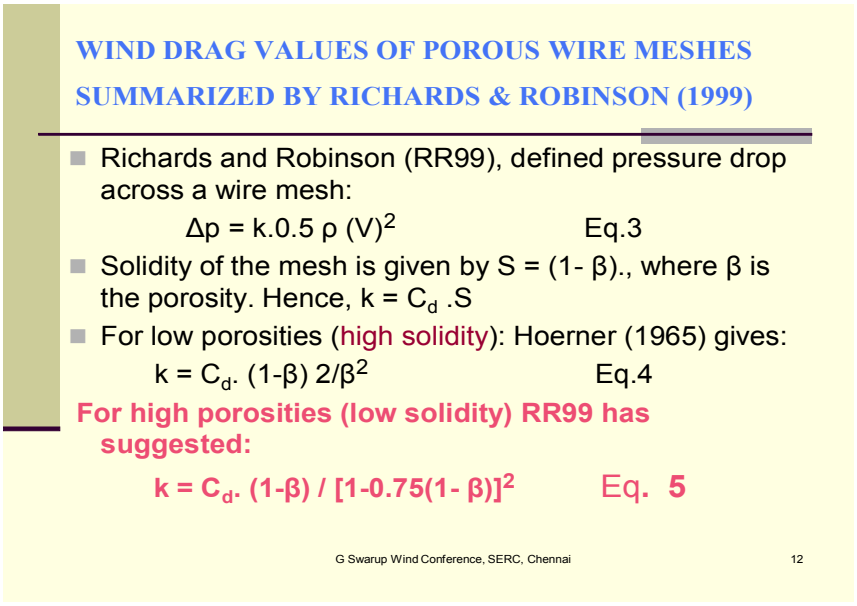

Fig. 5(c): Equations Giving Wind Drag Values of Porous Wire Meshes (RR99)

In Table II, is given comparison of calculated values of C_d using Eq (5) as above with values for various values of solidity of rectangular wire meshes of round wires measured by NAL (Jayraman 1987), Koppen (1987), Wyatt (1964) and Cohen (1964: the paper did not give wire mesh size), (see Swarup 2007). For the 6mmx6mmx0.55mm wire mesh, I have added in Table II measurements made by NAL (Jayraman 1987) and SERC-Chennai (Lakshman et al. 2008). **It is seen that the NAL values are consistent with those calculated by me using the equation of Richards and Robinson**. Also, see Fig. 3 of Swarup 2007.

Table II. Comparison of *calculated values* of Drag Factor,Cd, using Eq (5) of Richards and Robinson with *measured values* for various values of solidity of wire meshes of round wires

No.	Mesh size mm	mm	mm	Solidity	Cd Calculated	Cd Measured	References
1.	20	20	0.55	0.028	1.00	0.98	NAL(1987)
2.	15	15	0.55	0.072	1.11	1.07	NAL(1987)
3.	12	12	0.55	0.090	1.15	1.23	NAL(1987)
4.	10	10	0.55	0.107	1.17	-	
5.	6	6	0.55	0.175	1.32	1.30-	NAL(1987)
6.	15	15	1.4	0.178.	1.33	1.46	Koppen (1987)
7.	7.87	7.87	1.1	0.264	1.55	1.50	Wyatt (1964)
8.	---					1.30	Cohen (1964)
9.	6	6	0.55	0.175	1.32	1.00	SERC-Chennai

As described in Section 5.3, wind tunnel measurements have also been made on a wire mesh panel of spacing 6mm x 6mm made of 0.56m wires by the Structural Engineering Research

Centre (SERC) at Chennai (2007). They derived $C_d \sim 1.0$ for that mesh and a $\text{Cos}^2\ \theta$ variation with the wind direction up to $\sim 90^0$ (Fig. 4). The value of C_d by SERC is also tabulated in Table as serial no. 9.

Hence, I recommend that we should adopt <u>calculated</u> values of C_d as per serial 1 to 5 of Table II given in this Report, and also $\text{Cos}^2\ \theta$ variation for C_d as a function of θ of the wind direction with respect to the normal (or to be a bit conservative as Cos θ), for the proposed replacement of the present wiremesh mesh, as discussed in Section 6. Further, it may be prudent to get SERC measurements verified regarding calibration done by them by correspondence and perhaps also an independent measurement at the IIT Kanpur where there also exists a large wind tunnel.

6 Proposed Improvement of the Reflecting Surface.

6.1 *Design Considerations for the 45m dish*: As highlighted earlier, the design and economics of a parabolic dish is primarily determined by wind loads at survival velocity on its reflecting surface. In order to minimize wind loads on the GMRT dishes operating at m and dcm wavelengths, we decided to use wire mesh of low solidity (high porosity) for the reflecting surface. Since winds come from a horizontal direction, the wind load is obviously largest when a parabolic dish is pointed towards the horizon, and wind load is much lower when the dish is pointed towards the zenith. It is a general practice universally that parabolic dish antennas are rotated towards the zenith and stowlocked when the velocity exceeds, say 90 kmph; it is then assured that that the axial and bending stresses in the structural members due to 'dead loads' and wind loads at the survival wind velocity do not exceed allowable stress as per the National codes for civil and structural engineering (e.g. Indian Standard Institute codes IS800, IS875). The peak stresses are specified to be < 0.65 of the yield strength of the structural steel. However, after consultation with TIFR, TCE allowed 33% additional increase over the value of 0.65 in stress in any orientation of the 45m dishes, in the unlikely event that the 45m dish may not get stowlocked or pointed towards the zenith, as wind velocity rises to more than ~ 50 kmph during a summer thunderstorm (see TCE detailed design note DDN-5). From a perusal of the computer outputs (dated 1990) by TCE who tabulated stresses in about 4099 structural members of the 45m dish of the GMRT for different orientation of the dishes, subject to both dead loads and wind loads for a velocity of 133kmph, I find that 33% increase has been indeed found to apply for certain sections of the PRFs, for the case when the dish is pointed away from zenith by more than 30 degrees up to 75 degrees from the zenith. **At Pune (and northern India), the maximum wind exceeding 90 kmph occur ONLY during thunderstorms, mostly in summer months. During a very severe thunderstorm, wind velocity has been observed to rise up from ~ 50 kmph to 120kmph at the Shimla office of IMD in only 10 to 15 minutes. Hence, wind meters have been installed at each of the 45m dishes and antennas are required to be parked automatically to zenith when the wind velocity exceeds 45 kmph (1 min average).**

6.2 *Existing Wire Mesh of the Reflecting Surface of 45m dishes:* As described in Section 2, the GMRT antenna consists of 16 parabolic frames, called PRFs, connected to a Hub at inner end and to a "Rim" at outer extremes (Fig 1a.). Rope trusses of 4mm diameter are stretched between adjacent PRFs and then pulled back by rope trusses attached to the corresponding lower part of each subsection of PRFs (Fig.1b), so that the two intermediate nodes of the rope trusses also lie on the parabolic surface, same as the nodes at the top tubes of the PRFs. There are 12 rope trusses between the Rim and the Hub and 4 inside the Hub. The wiremesh of various sizes are tightly connected to the 4mm rope trusses using thin wires. As also described earlier, the existing reflecting surface of the 45m diameter parabolic dishes of the GMRT consists of stainless steel wire mesh of size 10mmx10mmx0.55mm for the inner one third area of the dishes, 15mmx15mmx0.55mm for the middle one third area and 20mmx20mmx0.55mm for the outer one third area. Fig. 6 shows a part of the plan of the 45m dish showing two adjacent parabolic frames.

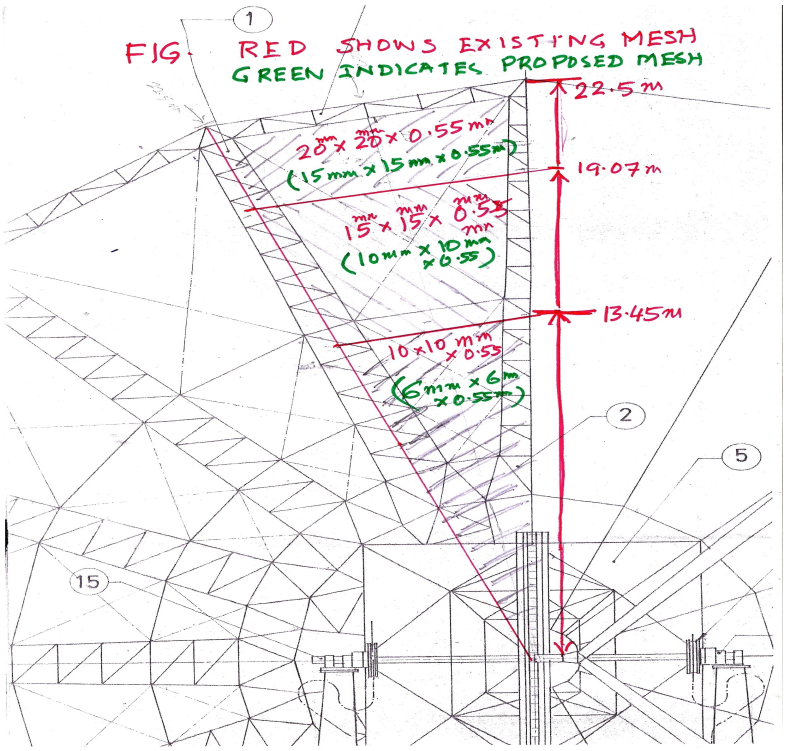

Fig. 6: shows a cut view of the Plan of the 45m dish of the GMRT, indicating in red that 10mmx10mmx0.55mm mesh has been installed presently from the centre of the dish to a radius of 13.45m, 15mmx15mmx0.55mm mesh from 13.45 to 19.05m and 20mmx20mmx0.55mm from 19.05 up to 22.5m (centre of the dish). In the brackets are shown proposed replacement of the above wire meshes by 6mmx6mmx0.55mm for the inner, 10mmx10mmx0.55mm for the middle and 15mmx15mmx0.55mm for the outer portion.

6.3 *Proposal* ***for Replacement of present wire meshes with finer Wire meshes*****: Considering that recent measurements show an appreciably lower value of C_d than that used by TCE during the design of the GMRT in 1998-89, I examine in this Report a possibility of using finer wiremesh of size 6mmx6mmx0.55mm for the inner one third areas of each dish, 10mmx10mmx0.55mm for the middle one third area and 15mmx15 mx0.55mm for the outer one third area as shown in Fig. 6 in brackets. I must stress that my calculations are rather approximate and only a detailed computer analysis by a structural engineer will be able to critically examine this proposal.**

Col. 2 of Table III gives solidity S of wire meshes of different sizes, $S = [1- (w-d)^2/w^2]$, where w = the width of the square mesh and d is diameter of the wire; Col. 3, gives C_d (TCE), values of the drag factor used by TCE for design of the GMRT; Col. 4 gives S x C_d ; Col. 5 C_d (GS) gives values used by me in this Report for the proposed reflecting surface and Col. 6 gives S x C_d .

Table III gives values of drag factor, C_d, and solidity S for wiremesh of different sizes

Wiremesh size	Solidity,S	C_d (TCE)	S x C_d (TCE)	C_d (GS)	S x C_d (GS)
20mmx20mmx 0.55mm	0.05424	1.45	0.078648	not used new proposal	
15mmx15mmx 0.55mm	0.07199	1.45	0.104386	1.05	0.075589
10mmx10mmx 0.55mm	0.10698	1.45	0.155121	1.1	0.117678
6mmx6mmx 0.55mm	0.17493	1.45	0.253649	1.3	0.227409
		(6mm not used presently)			

I have then calculated values of wind loads for each of the 12 rope truss segments from the Hub to the Rim. Col.1 of Table IV gives distance from the centre of the 45m dish for the outer, middle and inner areas. Col. 3 gives Dead Loads on a Rim and 12 sections of PRF (Type I) as calculated by Gerald Sequria of NCRA. In Col. 4 are given Wind Loads, WL, on Rims and 12 sections of PRF (Type I) at **37m/s x 1.15 for the height factor as per IS875**. The values of WL have been calculated by me as WL (kg/ m^2) = (0.5. ρv^2 .1m^2. S. C_d)/9.81, where ρ = air density = 1.106 kg/m^3 at the 650m site of the GMRT (Janardhan et al. 1990). In Col. 5 (A) are given EXISTING size of the wiremesh in the outer 1/3rd, middle 1/3rd and inner 1/3rd area of a 45m dish. In Col. 6 are given calculated values of the wind loads WL(A) using the calculated solidity and a wind drag factor C_d =1.45 as assumed by TCE for $\theta = 90^0$ (Janardhan et al. 1990). In Column 7 (B) are given proposed replacement of wiremesh of the proposed smaller sizes described above. Based on recent data (Table III), **I have assumed C_d = 1.05, 1.10, and 1.30**

for the 15mm, 10mm and 6mm mesh respectively. Calculated wind loads WL(B) for the specified wiremesh of Column 7 are given in Column 8.

Table IV: Cols. 3 and 4 gives Dead Load and Wind loads for the Rim and each of the 12 sections of PRF-Type I from the Rim to the Hub; Col. 5 give size of the existing wire mesh for each section and Col. 6 wind load for the existing mesh under under WL(A) and Cols. 7 gives the size of the proposed replacement of the wiremesh under, and Col. 8 wind load under WL(B). Col.3:Gerald, Col.4.TCE DDN: v02, sheet7:F2i x 0.55 x$(37x1.15)^2$/9.81; Col. 5 to 8 by G. Swarup using TCE DDN: V10, sheets 12 and 13).

Table IV

Col. 1	2	3	4	5	6	7	8
	Rim/	DL	WL	(A)	WL(A)	(B)	WL(B)
Radius	PRF no.	Rim/PRF Kg	Rim/PRF Kg	Wiremesh Size	Wiremesh Kg	Wiremesh size	Wiremesh Kg
22.50 m to 19.07 m	Rim	350	280	20x20x0.55		15x15x0.55	
	W1	47	43	Do	77	do	75
	W2	47	42	Do	73	do	70
	W3	47	43	Do	68	do	66
19.07 m to 13.45 m	W4	50	44	15x15x0.55	86	10x10x0.55	97
	W5	51	48	Do	80	do	90
	W6	54	49	Do	74	do	84
	W7	61	57	Do	69	do	77
	W8	71	60	Do	63	do	71
13.45 m to centre	W9	72	55	10x10x0.55	84	6x6x0.55	123
	W10	74	57	Do	75	do	110
	W11	91	66		66	do	97
	W12	91	89	Do	57	do	84
	Hub top (hub+mesh inside Hub			Do		do	
	1--2			Do	26	do	43
	2--3			Do	17	do	25
	3--4			Do	15	do	22
	4--5			Do	15		22

It is seen from Table IV that the maximum loads for the assumed survival wind speed of 37m/s x 1.15 factor for 25m height, are much higher than the DLs and WLs of the PRFs, particularly for the more

distant sections of the PRFs. It is also seen from Table IV that the wind loads for the proposed mesh sizes of lower spacing are nearly the same for the outer and middle portions of a 45m dish but appreciably higher for the inner 1/3rd portions for the case of 6mm mesh . On the other hand, it is known that the Bending Moment on the Hub that is supported by the cradle would depend on the wind load x distance of the application of the wind load. We may also note that a relatively large wind load of 280 kg (at a wind of 37m/s x 1.15) gets applied to the RIM at a distance of ~ 16 m from the Hub. We next examine in Section 6.4 resulting forces and bending moments for the case when the 45m dishes are pointed towards the horizon.

6.4 *Resulting forces on parabolic frames:* We now estimate resulting forces on the parabolic frames when the dish is subjected to a wind velocity of 133kmph x 1.15 (37m/s x 1.15). In the SMART design, the wiremesh is connected to 4 mm diameter stainless steel wire ropes that are stretched under tension between adjacent sub-sections of the parabolic frames (Fig.1). Initial tension increases considerably when the wind is exerted on the wire mesh by front wind i.e. towards the parabolic dish. The tension decreases for the case of the wind towards back of the dish. Initial tension in the 4mm ropes was selected by the TCE so that the tension in the wire ropes do not slacken except marginally, in case of the 137kmph x 1.15 (37m/s x 1.15) survival wind towards the back. For the case of front wind, the selected strength of the rope trusses allowed a safety factor of ~ 3 (see DDN v10).

Each of the rope truss (e.g. CRT 1) exerts a force in a direction that is perpendicular to the top members of the parabolic frames, called by TCE as "Radial Force", whence

F = 2T Sin 11^0.25 (DDN v02, v10, TCE…/153-DISHCRAD: pages 35-43, NCRA-Lib).

In Col. 4 of Table V are given values of the initial tension, T, calculated by the TCE that were executed during construction of the 45m dishes. Col. 5 gives increase of the tension for the case with wind velocity of 37m/s x 1.15 (maximum operational wind after antennas are parked at zenith and 23m/s all other positions); Col. 6: maximum expected tensions for the case of survival wind of 37m/s x 1.15 in any position, particularly when the dish is towards the horizon. Columns 7, 8, and 9 give calculated forces, F, in a direction perpendicular to each PRF (called 'Radial' direction by TCE). **It is seen that the maximum loads for the assumed survival wind speed of 37m/s are much higher (two to three times higher) than the DLs and WLs as given in Table IV for each of the 12 sections of the PRFs. LAST 3 columns are relevant.**

Table V: gives Tensions for V = 37m/s for the case when some ropes slacken								
Case A : 45m dish parked at zenith; Case C: all positions,								
1	2	3	4	5	6	7	8	9
			Initial	Case A	Case C	Radial	Radial	Radial
			Tension	Tension	Tension	Force	Force	Force
						Initial	CaseA	CaseC
Radius	Rope Truss	PRF			kg		kg	kg
22.50m	Rim							
outer	CRT1	W1	216	274	403	84	107	157
"	CRT3	W3	223	274	535	87	107	209
19.07m	CRT4	W4	232	280	521	91	109	203
middle	CRT5	W5	239	283	492	93	110	192
1/3rd	CRT6	W6	242	283	462	94	110	180
"	CRT7	W7	248	286	567	97	112	221
"	CRT8	W8	251	286	652	98	112	254
13.45m	CRT9	W9	254	289	577	99	113	225
Inner	CRT10	W10	258	293	557	101	114	217
1/3rd	CRT11	W11	261	293	530	102	114	207
"	CRT12	W12	261	299	340	102	117	133
"		inside Hub						
"	CRT13	1--2	232	280		91	109	110
"	CRT14	2--3	261	328		102	128	194
"	CRT15	3--4	261	328		102	129	218
"	CRT16	4--5	261	356*		102	139	162
0m(centre)								
*=Tabulated by GS using data TCE.../153-DISHCRAD: pages 35-43(NCRA-Lib)								
Factor of Safety (4mmRope): 4.8				3.5				

TableV: Col. 1 gives distance of the rope trusses and PRFs from the centre of the dish. Col. 2 gives the name of the rope truss and Col. 3 name of the concerned PRF sub-section, Col. 4: initial tension at the time of erection of 45m dish; Col.5 (Case A): increase in the tension during the wind velocity of 37m/s (maximum operational wind after antennas are parked at zenith and 23m/s all other positions); Col. 6 (Case C): maximum expected tensions for the case of survival wind of 37m/s in any position (particularly towards the horizon), Cols. 7, 8, and 9 give calculated Radial force, F, in a direction perpendicular to each PRF (called 'Radial' direction by TCE). It is seen that the maximum loads for the assumed survival wind speed of 37m/s are much higher (two to three times higher) than the DLs and WLs as given in Table IV for each of the 12 sections of the PRFs. LAST 3 columns are relevant.

6.5 *Resulting forces on parabolic frames when the dish is subjected to the wind velocity of 133kmphx 1.15 (37m/s x 1.15)*: A comparison of Tables V and IV show that the maximum loads for 37m/s x 1.15 wind speeds are much higher for Table V than the DLs and WLs in Table IV for each of the 12 sections of the PRFs. This is simply because the initial tension in rope trusses has been designed for supporting the wire meshes adequately against the survival wind. The load on the PRFs would be similar or higher, if the wire meshes were to be supported on steel trusses as in a conventional design. I have examined the possibility of using a simple back up structure using e.g. MS or Al channels and angles only for the portion up to a distance from the centre up to ~13.6 m in order to decrease the adverse effect of the considerable increase of radial forces (perpendicular to the triangular section of PRFs), particularly for the new proposal of using 6mmx6mm mesh in the inner portion. That proposal is not discussed here and would require discussions with a structural engineer.

In Table VI, I have calculated values of the Bending Moments (BM) at the Hub (Cols. 5 & 6) due to the Rim and different sections of the PRFs. For the present I have calculated only that part of the dish which is outside the Hub. The sum of the Bending Moment on PRF at the Hub due to the wind of 37m/s (Case C) is given by two parts: (a) the relatively large wind load on the Rim and (b) by the radial Forces on various sections of the PRFs as tabulated in Col. 3 of Table VI, multiplied by the distance of the applied forces from the Hub (Col. 4).

I have then estimated additional increase in the Bending Moment, BM that may result if we replace the wire meshes of smaller sizes as proposed. Since the values of WL with new estimates of C_d (Table III) are nearly the same for the 15mmx15mm and 10mmx10mm wire meshes as compared to the existing 20 mmx20mm and 15mmx15mm wire meshes respectively (Table IV), I have multiplied by a factor of 1.5 values only those areas of the wire meshes that are closer to the Hub (Col 7) for which the existing 10mmx10mm mesh is to be replaced by 6mmx6mm mesh.

As may be seen from Table VI (Col. 8), the new proposal will result in an increase of BM at the HUB by only about 5% and correspondingly similar increase in the stress in the tubes of the PRFs by only about 5%. As stated earlier, only a detailed computer analysis will be able to make a correct evaluation.

Table VI is given on the next page. A summary is given in the introduction and conclusions.

Table VI								
1	2	3	4	5	6	7	8	
		Radial	Distance	Bending				
		Force	d= from	Moment				
		F, Case C	Hub	F x d	total			
Existing		kg	m	kg.m	kg.m			
Wiremesh	RIM Wind	Load 280	15.85	4438				
Size		157	14.63	2297				
		183	13.4	2452				
20x20x0.55		209	12.18	2546				
do		203	10.96	2225				
do		192	9.74	1870				
do		180	8.52	1534				
15x15x0.55		221	7.3	1613				
do		254	6.08	1544	20519		20519	
do		225	4.86	1094		1094x1.5=	1641	
do		217	3.65	792		792x1.5=	1188	
do		207	2.43	503		503x1.5=	754	
10x10x0.55		133	1.22	162	23070	162x1.5	243	
do							24345/23070	
do				Percentage increase of BM =			1.0553	
do		110	0					
		194	1.22					
Not considered BM b		218	2.43					
inside Rope Trusses		162	3.65					

Table VI : Column 1, gives wire mesh size, Column 2 Rim WL, Column 3 Radial Force, Column 4, Distance from the Hub, Column 5, Bending Moment, Column 6, Total Upto 15 mm Mesh, Column 7: Column 5 x 1.5, Column 8, Total

7 Efficiency of a Parabolidal Antenna and of the GMRT at L band

7.1 *Efficiency of a parabolidal antenna:* There are several factors that determine efficiency of a paraboloidal antenna (Kildal 2000.):

1. Efficiency due to the spillover of the radiation pattern,
2. Efficiency due to the illumination radiation pattern and its taper,
3. Polarization efficiency,
4. Body of revolution loss (BOR) efficiency.
5. Phase efficiency,
6. Reflection loss at the input of the horn.

The designer of the antenna feed that is placed at the focus of the dish attempts to minimize spillover beyond the outer boundary of the dish and attempts that taper is such that illumination efficiency is as high as practical, by making the radiation pattern rather humped (see Fig. 8).

For a good primary feed, such as the Australian Feed for the GMRT or the South African proposed feed, the product of the first two terms should be about 70%. Polarization efficiency may be better than 95%. *The RRI L band feed is quite poor compared to the modern feeds, as discussed in Section 7.2.*

7.2 **I reproduce here a description of efficiencies for the Chalmers broadband feed (ref. …):**

"Efficiencies averaged from 0.3-1.7 GHz; (53^0 half angle):

Taper	78.2%
Spillover	88.9%
Phase	97.6%
Pol SL	91.6%
BORi	90.8%
Aperture	56.4%
Norm F02	72.9%

$$e_{ap} = e_{BOR1}\, e_{sp}\, e_{pol}\, e_{ill}\, e_{\varphi} \qquad \text{Eq.4.}$$

Where each of the sub efficiencies is explained below. The BORl (Body of Revolution) efficiency e_{BORI} measures how closely the far-field resembles that of a BORl antenna [Kildal 1985, 2000]. The far-field of a BORl antenna has only first order variation in $< \theta, \Phi >$ and can be expressed as

$$\mathbf{Gy}(\theta,\Phi) = \mathbf{G_E}(\theta)\,\mathbf{Sin}\,\Phi\,.\theta\hat{} + \mathbf{G_H}(\theta)\,\mathbf{Cos}\,\theta.\Phi\hat{} \qquad \text{Eq. 5.}$$

for the y-polarized case. The BORl efficiency accounts for the power radiated in higher order $< \theta, \Phi >$ variations in the pattern, which cannot contribute to the gain of a symmetrical reflector antenna and thus represents a power loss. The spillover efficiency $\boldsymbol{e_{sp}}$ is the fraction of the radiated power that actually hits the reflector. The power lost in the cross-polar part of the field is

accounted for by the polarization efficiency e_{pol}. The illumination efficiency e_{ill} is a measure of the loss that arises from the actual tapered illumination of the reflector, and finally the phase efficiency e_{φ} accounts for the loss due to phase errors in the co-polar field. This efficiency is the only efficiency that depends on the location of the feed relative to the focal point of the reflector. The feed location that maximizes the phase efficiency defines the phase center.

From the measured data available we can only compute the illumination- spillover- and polarization sub-efficiencies. These efficiencies are fortunately the main contributors to the aperture efficiency as the BORl efficiency and the phase efficiency usually are close to 0 dB. They are, for the Chalmers feed typically in the order of 0.1 dB." One should also consider return loss and any conduction loss of the feed.

7.3 *Low Frequency Quad Ridge Horn Feed:* Akgiray and Weinreb (2010) have developed a broadband feed for parabolic dishes covering the frequency range of 300MHz to 2000MHz. They have calculated efficiencies as follows; I reproduce only factors for the frequency range of 500 MHz to 1700 MHz :
*Taper= 75.*3%; Spillover = 91.1%; Phase = 99.1%; Pol SL = 80.1%; BOR1=87.1%; Aperture = 47.4%. (norm FoM =68.4%: I am (GS) not clear as to the meaning of FoM).

7.4 *Efficiency of Australian feed for the GMRT:* Granet et al. (2005) have designed a broadband feed for the GMRT to cover the frequency band of 550MHz to 900 MHz using a coaxial waveguide and a short OMT. They have calculated efficiency of ~ 70% for most of the above range. It is not clear whether they have considered polarization efficiency, BOR and return loss. Nevertheless, it has good performance. A feed has been fabricated and tests are being made on one or more of the GMRT antennas and also at a new test range at NCRA.

7.5 *The RRI's L-band feed installed on all the 30 antennas of the GMRT:* A detailed description of the wideband corrugated horn, orthomode transducer and low-noise amplifier is given by A. Raghunathan in his M. Sc. Eng (by research) thesis to Bangalore University dated 2000 (NCRA/TIFR library acc no. 11808). We reproduce below a few highlights.

7.5.1On page 26 of his M.Tech. thesis, Raghunathan has given E and H plane radiation at 1000, 1200 and 1400 MHz. As can be seen from Fig. 7 that E and H patterns are nearly the same at 1420 MHz but there is considerable difference at the lower frequencies. It is clear that this feed has poor polarization characteristic at 1000 and 1200 MHz but seems good at 1420MHz

GMRT L band Feed: E and H Plane Radiation patterns

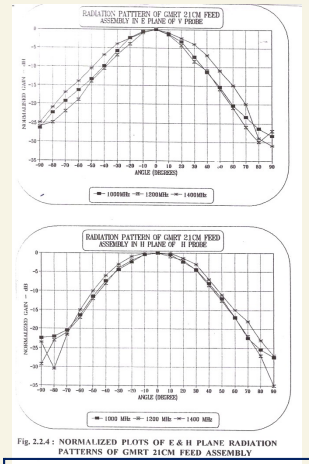

Fig. 2.2.4 : NORMALIZED PLOTS OF E & H PLANE RADIATION PATTERNS OF GMRT 21CM FEED ASSEMBLY

Fig…Copied from Raghunatahan's thesis (2000): upper fig. E plane and lower fig. H plane

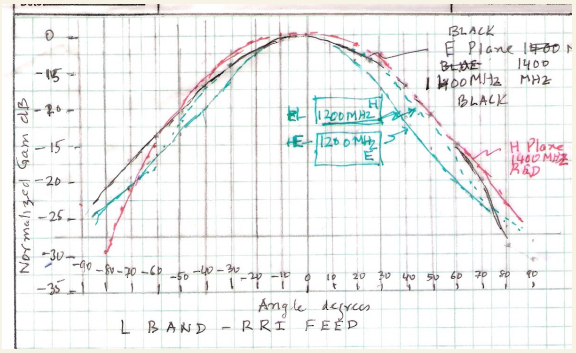

E and H plane radiation patterns superimposed for 1400 MHz and 1200 MHz (by G. Swarup). E and H close at 1400 MHz with -15 dB taper at 62.5 degree but at 1200 MHz -17 dB taper.

Fig. 7: gives a comparison of the radiation patterns of RRI L band feed:

7.5.2*:* Return Loss of the L band feed of RRI varies from -10 to -15 dB that is good. However, insertion loss varies from about 0dB to 0.5 db but mostly less than 0.2 dB in the above frequency range (p. 30 of Raghunathan's thesis).

7.5.3*:* System Temperature and Dish Efficiency: I reproduce in Table VII below the values described by Raghunathan at the GMRT at 4 frequencies:

Table VII: Efficiency and A_{eff} of the L Band feed of the GMRT designed by A. Raghunathan based on his measurements on one of the GMRT antennas. (Antenna no. is not given in his thesis).

Frequency (MHz)	System temperature (K)	Dish Efficiency (%)	Effective Area* A_{eff} m^2
1000	53	38	604
1170	54	33	525
1280	63	35	557
1390	71	33	525

*Aff = A_{phy} x efficiency = $\Pi D^2/4$ = 1590 x efficiency.

7.6 In Fig.8.is given a comparison of the radiation patterns of the RRI L band feed at 1400 MHz with, the S. African feed and the Kildal 327 MHz feed of the GMRT. The 327 MHz feed has a flat top radiation pattern that would result in higher illumination efficiency. It may be worth fabricating one for the L band, particularly the design of the improved 327 MHz feeds that have bandwidth of ~ 1.7 or better.

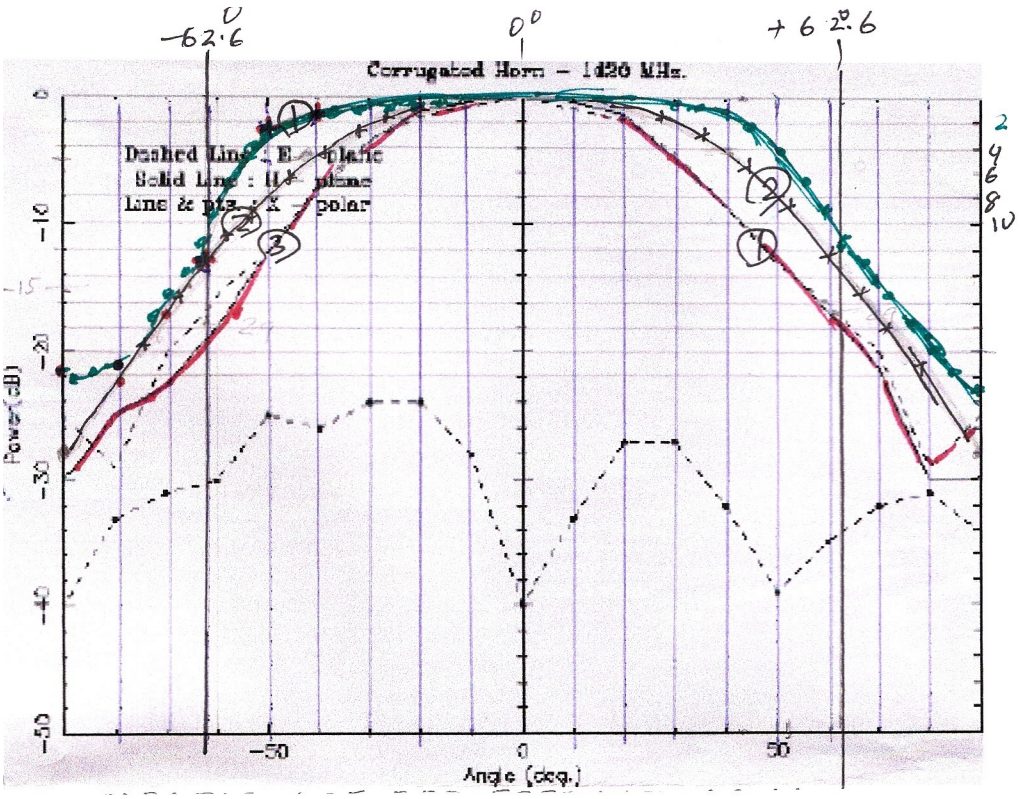

Fig.8. gives comparison of the radiation patterns of the RRI L band feed at 1400 MHz (Curve 1 in red), S. African feed (Curve 2 in blue) and the Kildal 327 MHz feed of the GMRT (Curve 3 in green). The 327 MHz feed has a flat top radiation pattern that would result in higher illumination efficiency. It may be worth fabricating one for the L band, particularly the design of the improved 327 MHz feeds that have bandwidth of ~ 1.7 or better.

7.7 *As can be seen from the brief data given in Sections 7.1 to 7.6, it should be possible to get a new feed designed for the L band of the GMRT so that the 45m dishes have efficiency of at least 50%, including rms errors (see Section 6 regarding my proposal for improvement of the reflecting surface)*. Also, a well designed feed will minimize spillover radiation and thus decrease contribution to the system temperature, apart from lower leakage through the mesh as per Section 6. The proposed South African feed will even allow operation of the L band from 1000 MHz to ~ 1750 MHz, of importance for studies of: (a) OH megamasers, (b) polarization studies of radio galaxies and quasars and (c) search towards Galactic plane and also dispersion measurements of pulsars. At present, GMRT sensitivity (A_{eff} / T_{sys}) is much poorer compared to that of Arecibo by nearly a factor of about 2.5 or 3 . The new L band feed will make the sensitivity of the GMRT to be within a factor of ~1.5 or so of that of the Arecibo and of course the GMRT has very much higher resolution than that of the 300m diameter fixed Arecibo dish, for which only ~ 200m of the dish is illuminated to allow tracking over +/- ~2 hours, and that covers only a declination range of ~0^0 to 40^0. In contrast, the GMRT 45m dishes cover a declination range of ~ -53^0 to + 90 degrees and allows tracking for +/- 5 hours or so. In my view, it would take more than a decade when phase I of the SKA would start exceeding the improved GMRT in the L band. Besides, GMRT could be used for make deeper observations over few hundred hours for special projects, for which time may not be easily available with SKA.

8 Conclusion

Theodolite measurements of the reflecting surface of the 45m dishes of the GMRT made during 1993-96 have shown that the peak to peak deviations of the reflecting surface are much larger than were specified to the Contractors in the Work Order and contract signed in 1989. The larger rms errors have resulted in lower values of antenna efficiencies in the L band of the GMRT. The 'RMS efficiency' at 1420 MHz for 14 out of 15 antennas constructed by VMJ varies from ~ 56% to 96% with average of about 80%. For the SSL antennas data was analyzed by G. Sankar only for 7 antennas, with RMS efficiency varying from ~ 36% to 92%. It may be noted however that the RMS efficiencies are closer to 100% at 610MHz and lower frequencies because phase errors due to the surface deviations are inversely proportional to the square of wavelength. Correcting these deviations would result in appreciable increase in the effective collecting area of the dishes by > 20% at L band. Combined with a finer wiremesh and a new feed, efficiency of the GMRT at L band could increase by a factor of ~ 2.

It is also important to change the *rusted galvanized turnbuckles* that are connected to the rope trusses supporting the wiremesh panels by stainless steel units that have been developed by the GMRT maintenance engineers. Certain other urgent repairs to the tubular members of the parabolic frames are also required.

Wind loads or forces on a surface of an antenna are proportional to the drag factor, C_d. In 1987, measurements were made of the drag factor, C_d by Jayaraman (1987) at the National Aeronautical Laboratory (NAL), Bangalore on a request by TIFR, for the wire meshes of low solidity planned for the GMRT, with their C_d values being from ~ 1 for the 20mmx20mmx0.55mm mesh to 1.3 for 6 mmx6mmx0.55mm mesh . However, during the design of the GMRT antennas, TCE adopted C_d = 1.45 for all the 3 wire mesh sizes at normal incidence of the wind based on available literature and appreciably higher values as a function of departure

from normal to the mesh compared to the measured values of C_d at the NAL. Recently, Richard and Robinson (1999) derived an equation to fit values of C_d for wiremesh of different porosity/solidity, based on all the available information in the literature. Based on that equation, I have recently shown that the lower values of C_d ~ 1.0 to 1.3, for different mesh sizes, measured at the NAL confirm to their equation (Swarup 2007). Also, recent measurements on a 6mm x 6mm x 0.55 mm mesh made at the Structural Engineering Research Centre (SERC), Chennai have indicated a value of only 1.0 for the 6mmx6mmx0.55mm mesh. Hence, a proposal is made in this Report for replacing the present wiremesh with a wiremesh of smaller spacing. Presently the reflecting surface of the 45m diameter dishes of the GMRT consists of wire mesh of size 10mm x 10mm x 0.55mm for the inner one third areas of the dishes, 15mm x 15mm x 0.55mm for the middle one third area and 20mm x 20mm x 0.55mm for the outer one third area. Considering that recent measurements show an appreciably lower value of C_d than that used by TCE during the design of the GMRT in 1998-89, I have examined in this Report in some detail the possibility of using wire meshes of lower spacing i.e. of size 6 mm x 6mm x 0.55mm for the inner one third areas of the dishes, 10mm x 10mm x 0.55mm for the middle one third area and 15mm x 15 mm x 0.55mm for the outer one third area. My tentative conclusion indicates that the above proposal seems feasible but a detailed computer analysis would be necessary.

Wire meshes of lower spacing (size) would decrease the transmission loss, increasing reflectivity and also lower contribution to the receiver temperature by the radiation by the ground. Further, lower rms deviations *and a new L band feed* would result in appreciable increase in the sensitivity of the 45m dishes by a factor of ~2 at the L band, and also allow operation up to 1.7 GHz or higher.

It would be highly desirable to make the above changes in the next few years in a systematic way. All the above are major jobs and would need a suitable contractor. A budget of ~ Rs 5 or 6 or 10 crores could be planned in the 12th plan for improving the reflecting surface of the GMRT antennas and *also increasing reliability of the structural and mechanical parts of the dishes for a life of more than 30 years from now*.

9 Acknowledgement

I thank Shri S. C. Tapde and Shri G. Sankar for several discussions.

10 References

(Copies of several references listed below available at the NCRA/TIFR library, Pune 411007)

Akgiray, A. and Weinreb, S."Low Frequency Quad Ridge Horn Outline Drawings", California Institute of Technology, Los Angles, USA, 26 Aug 2010

Bracewell, R. N. "Tolerance Theory of Large Antennas", IRE Transactions on Antenna and Prpogation, 1961, pp. 49-58.

Cohen, E., Vellozzi, J. and Suh, S.S., “Calculations of Wind Forces and Pressures on Antennas”, Annals of the New York of Academy, 1964, Vol. 116, pp. 160-221, 1964. (Copy of Vol. 116 available at the NCRA/TIFR library).

Detailed Design Notes (DDN) for the Giant Metrewave Radio Telescope, Tata Consulting Engineers (TCE), ‘TCE-G18-01-153-v-00 to v11’, (Copy available NCRA/TIFR Library).

Janardhan, B., Yogi, M.K.S., Swarup, G., “Static and Dynamic Wind Load Considerations for a 45m Antenna With Wire Mesh Reflector”, Proc. Intl. Symp. “Experimental Determination of Wind Loads on Civil Structures”, Dept. Civil Engg., University of Roorkee, India, Oxford & IBH Publishing C., New Delhi, pp. 285-295, 1990. (Available NCRA/TIFR Library).

Granet,C., Davis, I.M., Forsyth, A.R., Bird, T.S., “Design of a Prime-Focus Dual-Band Feed for the Giant Metre-wave Radio Telescope”, Report No. 05/220, CSIRO, ICT Centre, PO Box 76, Epping NSW 1710, Australia, pp. 1-27, 2005.

ESDU 82031, “Paraboloidal Antennas: Wind Loading, Part I: mean forces and moments”. ESDU 82031, 1984, ESDU International Ltd., 251-259 Regent Street, London, W1R 7AD, (copy available at NCRA Library, Pune University Campus, Pune 411007)

Janardhan, B., Yogi, M.K.S. and Swarup, G., “Static and Dynamic Wind Load Considerations for a 45m antenna with Wire Mesh Reflector”, Proc. of the Intl. Symposium on “Experimental Determination of Wind Loads on Civil Structures”, held at New Delhi under the auspices of the University of Roorkee, Oxford & IBH Publishing Co., New Delhi, 1990, pp. 285-296.

Jayraman, V., “Wind Tunnel testing of Screen Elements Used for a Radio Telescopic Antenna (GIMRT)”; Fluid Mechanics Division, National Aeronautical Laboratory, Project Document FM 8723, October 1987, pages 1-7; 11Figures; Tables 1-20.

Kapahi, V.K. and Swarup, G., “Specifications of Extreme Wind Speeds at Narayangaon for the Design of the GMRT Antennas”, TIFR Centre Bangalore 560012, 1986, pp. 1-11, (copy available at NCRA Library, Pune University Campus, Pune 411007)

Kildal, P.S., “Factorization of the Feed Efficiencies of Paraboloids and Cassegrain Antennas”, IEEE Trans. Antennas & Propagation, Vol. AP-33, Aug 1985.

Kildal, P.S., “Foundation of Antennas-A Unified Approach”. Studentlitteratur, 2000, (copy available at NCRA Library, Pune University Campus, Pune 411007)

Koppen,C.J.W. Dr. “Summary of Mesh Report”: given to G. Swarup in 1987 by Dr. Ben Houghoudt of ASTRON, Dwingelow, Netherlands.

Lakshmanan, N., et al. “Wind Tunnel Studies on a Panel with a Wire Mesh/ Perforated Sheet for Dish Antenna”, Structural Engineering Research Centre, Chennai, CSIR, Project No. 600941 and 608941, dated July 2008, pages 1-26.

Raghunathaan, A., M. Sc. Eng (by research) thesis to Bangalore University dated 2000 (NCRA/TIFR library acc no. 11808)

Richards, P.J. and Robinson, M., "Wind loads on Porous Structures", J. of Wind Engineering and Industrial Aerodynamics, Vol. 83, pp. 455-465, 1999

Ruze, J., "The effect of Aperture Errors on the Antenna Radiation Pattern", Supplemento AL Volume IX, Serie IX del Nuovo Cimento, No. 3, 1952, pp. 364-380, 1952

Ruze, J., "Antenna Tolerance Theory-a Review", Proc. IEEE, vol. 54, pp. 633-640, 1990

Sivaramakrishnan, K., Yajnik, K. Jayraman, V., 'Wind Loads on Sparse Meshes used in Antennas of Large Radio Telescopes" Fluid Mechanics Division, National Aeronautical Laboratory, Project Document FM 8723, September 1988, pages 1-13.

Swarup, G., "Structural Design of the 45 m Diameter Antennas of the GMRT, Specifications, Summary of Analysis made by TCE, Safety Considerations and some Suggestions for the Proposed Review by TCE", ITR 236, NCRA Library, Pune University Campus, Pune 411007

Swarup, G."Wind drag factors for low solidity wire-meshes for parabolic dish antennas", in Proc. Fourth National Conference on WIND Engineering, NCWE-2007, held at Structural Engineering Research Centre, Chennai, 30th Oct-1st Nov, 2007, Eds. N.Lakshmanan, Arunachalam, S., Gomathinayagam, S., Allied Publishers, New Delhi, 129-136, 2007.

Tata Consulting Engineers (TCE), "Detailed Design Notes (DDN), v01-v11", 1989 (copy available at NCRA Library, Pune University Campus, Pune 411007)

Wyatt, T.A., "The Aerodynamics of Shallow Paraboloidal Antennas". Annals of the New York of Academy, 1964, Vol. 116, pp.222-238, 1964. (Copy of Vol. 116 available at the NCRA/TIFR library).

11 List of Figures and Captions

Fig.1(a): On left is shown a Plan showing 16 parabolic frames, (PRFs) of the 45 m dish, that are connected at the outer end to 16 RIMs, and on inner side to a central HUB. The HUB is connected to to a cradle (not shown here) that is palced on two elevation bearings palced on a Yoke.

Fig. 1(b): On the right is shown connestion of the reflecting surface. The outer part of each PRF from the Hub to the Rim consists of 16 sections. At each of the 16 sections, stretched ropes are connected between adjacent PRFs, as shown in the middle part of the Fig 1(b) marked by a double tick, and finally the wire meshes are stretched and connected to the rope trusses. The configuration shown in the bottom of Fig. 1(b) (on right side) was not adopted because of the possibility of oscillations of the stretched rope trusses..

Figure 2(a) Relative Efficiency at 1420 MHz of 14 out of 15 antennas constructed by VMJ; it may be seen that the antennas C3, C4, W5 and E4 have relative efficiency < 80% due to large RMS errors of the surface (see Table 1(a)).

Figure 2(b) Relative Efficiency at 1420 MHz of 7 out of 15 antennas constructed by SSL; it may be seen that the antennas E3, C10 and C13 have relative efficiency < 80% due to large RMS errors of the surface, with C13 being only ~36%! (Table 1(b).

Fig.3: Curve marked as 5 (red) shows variation of the Wind drag factor, C_d with angle of incidence of the wind as adopted by TCE for **all the three wiremesh of the GMRT**, with value at normal incidence to the mesh as $C_d \sim 1.45$. Curves, A, B and C (black) show wind tunnel measurements made at NAL, Bangalore in 1987. Curve D (blue) shows wind tunnel measurements made at SERC, Chennai, on a wiremesh of size 6mm x 6mm x 0.55mm,….

Fig4: Measurement of Drag factors by Lakshmanan et al. (2008) of SERC, Chennai.

Fig. 5(a): plotted by Richard and Robinson (1999) shows that C_d has dependence between Cos θ and Cos^2 θ.

Fig. 5(b). Loss coefficients k for round wire mesh screen shows that k has a non-linear relation: (Fig. 1 of RR99).

Fig. 5(c): Equations Giving Wind Drag Values of Porous Wire Meshes (RR99)

Fig. 6: shows a cut view of the Plan of the 45m dish of the GMRT, indicating in red that 10mmx10mmx0.55mm mesh has been installed presently from the centre of the dish to a radius of 13.45m, 15mmx15mmx0.55mm mesh from 13.45 to 19.05m and 20mmx20mmx0.55mm up to 22.5m. In the brackets are shown proposed replacement of the above by 6mmx6mmx0.55mm for the inner, 10mmx10mmx0.55mm for the middle and 15 mmx15mmx0.55mm for the outer portion.

Fig. 7: gives a comparison of the radiation patterns of RRI L band feed

Fig.8. A comparison of radiation pattern of the RRI L band feed at 1400 MHz (Curve 1 in red) with that of S. African feed (Curve 2 in blue) and with that of the Kildal 327 MHz feed of the GMRT (Curve 3 in green). The 327 MHz feed has a flat top radiation pattern that would result in higher illumination efficiency. It may be worth fabricating one for the L band, particularly the design of the improved 327 MHz feeds that have bandwidth of ~ 1.7 or better.

12 List of Tables and Captions

Table I (a) gives relative RMS efficiencies at 1420 MHz of 14 out of 15 antennas constructed by M/s V. M. J. Engineering Ltd., based on measured deviations over ~ 6000 points from a true paraboloid using a theodolite. It is seen that the antennas C3, C4, C9, W5, E4 and E6 have much lower efficiency, varying from ~ 55% to 84%. The overall relative efficiency is ~ 80%, implying the average value of the collecting area of these 14 antennas as $0.481 \times 0.8 \times \pi\ 45^2/4 = 611 m^2$. However, if we consider the value of the efficiency given by Raghunathan as 0.33 (see text), the average value of the collecting area at L band = 419 m^2.
Table I(b): gives as a typical example of the surface deviations from a true paraboloid of 27 points across the adjacent parabolic frames of the Sector 1-2 of the C9 antenna that was constructed by VMJ. Measurements were done by a surveyor of NCRA, using a theodolite and reduced by G. Sankar. Sector 1-

2 is one of the 16 sectors of the full 45m dish. Points marked as R1-1 and R9-3 refer to values measured on and near the adjustable blocks of the parabolic frames. R4-1 and R7-1 give deviations at the anchor points of the rope trusses (see Fig. 1). On the right side are given specified values as per the contract. It is seen that many values marked by shadowing are much larger than the values as per contract specifications resulting in reduced efficiency of the 45m dish.
Table I(c): RMS Efficiencies of 7 out of 15 antennas constructed by M/s Structural Steel Ltd., Madras (now Chennai).

Table II: Comparison of calculated values of Drag Factor, C_d, using Eq. (5) of Ricahards and Robinson with measured values for various solidity of wire meshes of round wires.

Table III gives values of drag factor, C_d, and solidity, S for wiremesh of different sizes.

Table IV: Cols. 3 and 4 gives Dead Load and Wind loads for the Rim and each of the 12 sections of PRF-Type I from the Rim to the Hub; Col. 5 give size of the existing wire mesh for each section and Col. 6 wind load for the existing mesh under WL(A) and Cols. 7 gives the size of the proposed replacement of the wiremesh under, and Col. 8 wind load under WL(B).

TableV: Col. 1 gives distance of the rope trusses and PRFs from the centre of the dish. Col. 2 gives the name of the rope truss and Col. 3 name of the concerned PRF sub-section, Col. 4: initial tension at the time of erection of 45m dish; Col.5: increase in the tension during the wind velocity of 37m/s (maximum operational wind after antennas are parked at zenith and 23m/s all other positions); Col. 6: maximum expected tensions for the case of survival wind of 37m/s in any position (particularly towards the horizon), Cols. 7, 8, and 9 give calculated Radial force, F, in a direction perpendicular to each PRF (called 'Radial' direction by TCE). It is seen that the maximum loads for the assumed survival wind speed of 37m/s are much higher (two to three times higher) than the DLs and WLs as given in Table IV for each of the 12 sections of the PRFs. LAST 3 columns are relevant.

Table VI: Col. 1 gives size of existing wiremesh, Col. 2 indicates Rim and PRF no. , Col. 3 gives calculated Radial Force F on PRF, Col. 4 its distance from the HUB, Col. 5 Bending Moment on PRF, Col. 6 total up to the distance of Col. 4, Col 7 approximate estimate of increase of BM by a factor of 1.5 for the case if the existing 10mmx10mm mesh is replaced by 6mmx6mm mesh, Col. 8 gives the total BM at the HUB. It is seen that the total BM increases only by a factor of ~ 1.05 for the proposed replacement of all the 3 wiremesh sizes.